Chapter 2

Basic Motion Planning

This Chapter makes the analysis of the geometric constraints of planar assembly tasks (two degrees of freedom of translation and one of rotation) for polygonal objects. This analysis is done in the configuration space and in the parametrized translational configuration space, which is an embedding of the rotational degree of freedom into the translational configuration space. As a result, an algorithm to compute the parametrized translational configuration space is presented. Then, the Chapter presents an exact cell decomposition method to plan the motions to move the manipulated object from an initial to a goal configuration. The Chapter is completed with an the study of the possible resulting reaction forces that appear when the contact situations take place.

2.1 Preliminaries

Let $\mathcal{A}$ and $\mathcal{B}$ be two polygons describing a manipulated object and an static object, respectively. Let $\{W\}$ and $\{T\}$ be the reference frames attached to the workspace and to the manipulated object $\mathcal{A}$, respectively. $\{T\}$ has the origin at the manipulated object reference point $\{O_{\mathcal{A}}\}$, and an orientation ϕ with respect to $\{W\}$. The vertices of $\mathcal{A}$ will be described with respect to $\{T\}$ by a vector $\vec{h}$, with module h and orientation γ. The vertices of $\mathcal{B}$ will be described with respect to $\{W\}$ by their x and y coordinates.

Two types of basic contacts can take place [62]:

Type-A: an edge of $\mathcal{A}$ against a vertex of $\mathcal{B}$.

Type-B: a vertex of $\mathcal{A}$ against an edge of $\mathcal{B}$.

The contact vertices will have a subindex indicating the basic contact to which they belong, i.e. (x_i, y_i) if the basic contact i is a type-A basic contact, and $(h_i \cos\gamma_i, h_i \sin\gamma_i)$ if it is a type-B basic contact.

Definition 1: *A contact situation* between two rigid polygonal objects is the occurrence of a single basic contact or the simultaneous occurrence of a given set of basic contacts.

Definition 2: The *set of contact orientations* R_ϕ^S of a contact situation involving a set S of basic contacts is the set of orientations for which the contact situation is possible, only considering the constraints imposed by the edges and vertices involved in any of the contacts of S.

Definition 3: The *configuration space* ($\mathcal{C}$-space) of a manipulated object is the space of all the possible configurations of the object, a configuration being the specification of the position and orientation of $\{T\}$ with respect to $\{W\}$ [69].

The $\mathcal{C}$-space is a smooth manifold of dimension $m = \frac{1}{2}N(N+1)$, N being the dimension of the workspace [62]. For movements in the plane with two degrees of freedom of translation and one of rotation, the $\mathcal{C}$-space is $\mathbf{R}^2 \times S^1_\rho$, where S^1_ρ is the circle of radius ρ, the gyration radius of the manipulated object. Then, any configuration is described by three generalized coordinates (x, y, q), with $q = \rho\phi$, all having units of length[1]. The x and y coordinates of the $\mathcal{C}$-space represent the translation of $\{O_\mathcal{A}\}$ with respect to $\{W\}$; therefore, the $\mathcal{C}$-space reference frame has the x-axis and the y-axis coincident with those of $\{W\}$.

If the orientation of the manipulated object remains fixed at a given orientation ϕ_0, the configuration space of the object is two-dimensional since only the two degrees of freedom of translation are to be considered. This translational configuration space is the section of the three-dimensional $\mathcal{C}$-space for the orientation ϕ_0.

Definition 4: The *parametrized translational configuration space* ($\mathcal{C}'$-space) is the space union of the translational configuration spaces for each possible orientation of the manipulated object.

The $\mathcal{C}'$-space can be obtained by projecting the $\mathcal{C}$-space on the xy-plane ($q = 0$), and associating to the projection of each section the value of its orientation, i.e. parametrizing the projection with the orientation [83]. Therefore the $\mathcal{C}'$-space reference frame coincides with $\{W\}$. By using this coincidence, the physical space will usually be drawn together with the $\mathcal{C}'$-space, which will help the understanding of the $\mathcal{C}'$-space.

2.2 One basic contact situations

2.2.1 Representation in configuration space

Definition 5: The *$\mathcal{C}$-face* $\mathcal{F}_i$ corresponding to a basic contact i is the set of configurations in the $\mathcal{C}$-space for which the basic contact takes place, only considering the constraints imposed by the edges and vertices involved in the basic contact, i.e. the contact edge and the adjacent edges to the contact vertex.

[1] Vector orthogonality in $\mathcal{C}$-space makes physical sense if ρ is the gyration radius of the manipulated object [38].

Definition 6: The *supporting cylinder* C_m^a associated to vertex A of $\mathcal{A}$ defined by $\vec{h}_a$, and to vertex M of $\mathcal{B}$ defined by (x_m, y_m) is a cylinder in the $\mathcal{C}$-space of radius h_a and axis parallel to the q-axis passing through the point $(x_m, y_m, 0)$.

Proposition 1: *The $\mathcal{C}$-face corresponding to a given basic contact is a ruled surface whose ruling segments are parallel to the xy-plane, have the same length that the contact edge and have their extremes on two helices over the two supporting cylinders associated to the involved vertices.*

Corollary 1.1: For a type-A basic contact between the vertex M of the fixed object and the edge of the manipulated object limited by the vertices A and B, the supporting cylinders are C_m^a and C_m^b, and the ruling segments are tangent to a cylinder concentrical with the supporting ones, and with radius equal to the distance in physical space from $\{O_\mathcal{A}\}$ to the line containing the contact edge. Figure 2.1b shows the $\mathcal{C}$-face corresponding to the type-A basic contact shown in Figure 2.1a.

Corollary 1.2: For a type-B basic contact between the vertex A of the manipulated object and the edge of the fixed object limited by the vertices M and N, the supporting cylinders are C_m^a and C_n^a, and the ruling segments are parallel. Figure 2.2b shows the $\mathcal{C}$-face corresponding to the type-B basic contact shown in Figure 2.2a.

Proof: If the manipulated object is translated keeping fixed its orientation and maintaining a given basic contact, the reference point describes a straight segment parallel to the contact edge and of its same length, i.e. in the $\mathcal{C}$-space it is a segment parallel to the xy-plane, being each of its extremes the configuration corresponding to the contact between the contact vertex and a vertex of the contact edge. When the manipulated object is in one of these configurations, i.e. a vertex (x_m, y_m) of the static object is in contact with a vertex $(h_a \cos\gamma_a, h_a \sin\gamma_a)$ of the manipulated object, and it is rotated around the contact point, the reference point describes the following curve in the $\mathcal{C}$-space:

$$\begin{aligned} x &= x_m + h_a \cos(\pi + \phi + \gamma_a) \\ y &= y_m + h_a \sin(\pi + \phi + \gamma_a) \\ q &= \rho\phi \end{aligned} \tag{2.1}$$

This curve is an helix supported by a cylinder C_m^a of radius h_a and axis parallel to the q-axis and passing through the point $(x_m, y_m, 0)$. ◇

Let us define:

ψ_T: the orientation with respect to $\{T\}$ of the normal to the contact edge.

ψ_W: the orientation with respect to $\{W\}$ of the normal to the contact edge.

d_W, d_T: the signed distances in physical space from the straight line that contains the contact edge to the origins of $\{W\}$ and $\{T\}$, respectively. If (x_e, y_e) is a point of the contact edge, then:

$$d_W = x_e \cos\psi_W + y_e \sin\psi_W \tag{2.2}$$

$$d_T = x_e \cos\psi_T + y_e \sin\psi_T \tag{2.3}$$

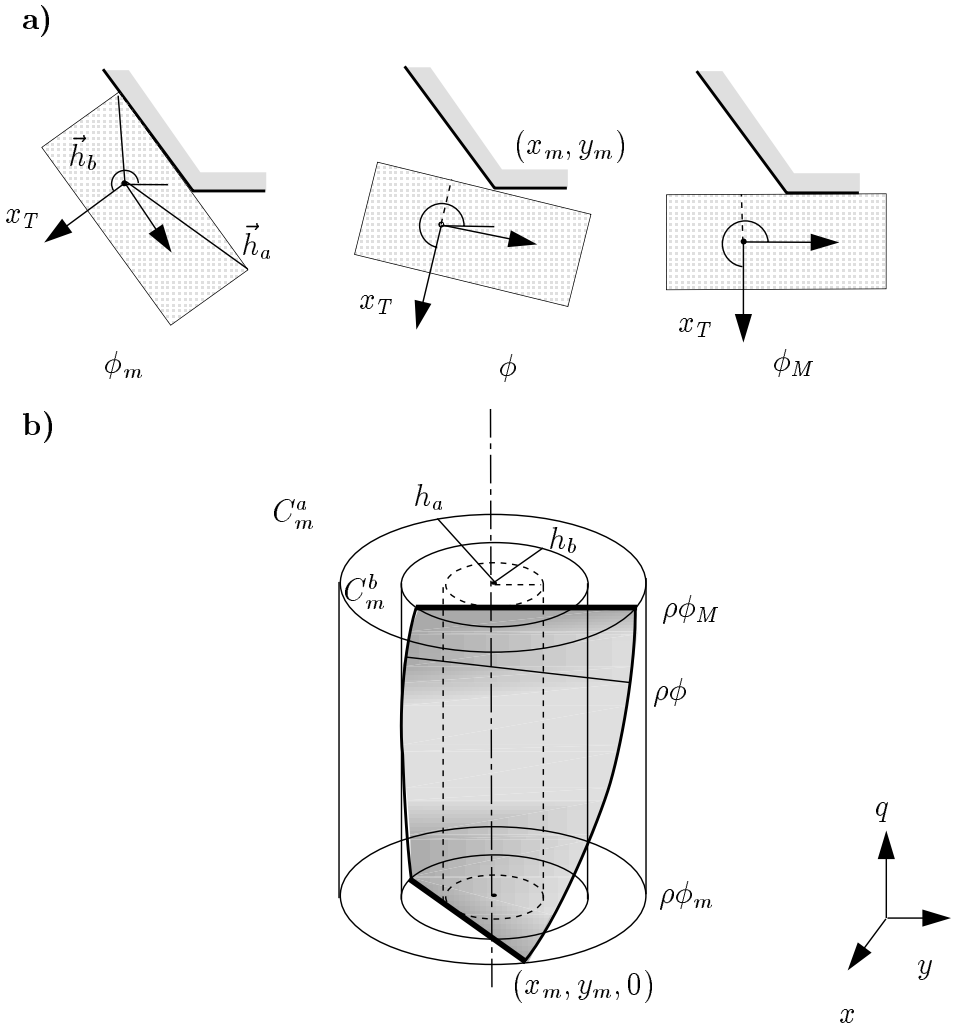

Figure 2.1: *Representation of a type-A basic contact in physical space (a) and in configuration space (b).*

D: the distance from the origin of $\{W\}$ to the projection on the xy-plane of the line that supports the ruling segment corresponding to a given orientation ϕ of the manipulated object. If a basic contact i is a type-A basic contact, then D is given by (Figure 2.3):

$$D = x_i \cos\psi_W + y_i \sin\psi_W + d_T \tag{2.4}$$

where (x_i, y_i) are the coordinates of the contact vertex of the fixed object measured in $\{W\}$ and ψ_W depends on the orientation ϕ of the manipulated object ($\psi_W = \psi_T + \phi + \pi$). Otherwise, D is given by (Figure 2.4):

$$D = h_i \cos(\psi_W + \pi - \gamma_i - \phi) + d_W \tag{2.5}$$

where h_i and γ_i are, respectively, the module and orientation of the vector defining the contact vertex of the manipulated object with respect to $\{T\}$, and ψ_W is independent of ϕ.

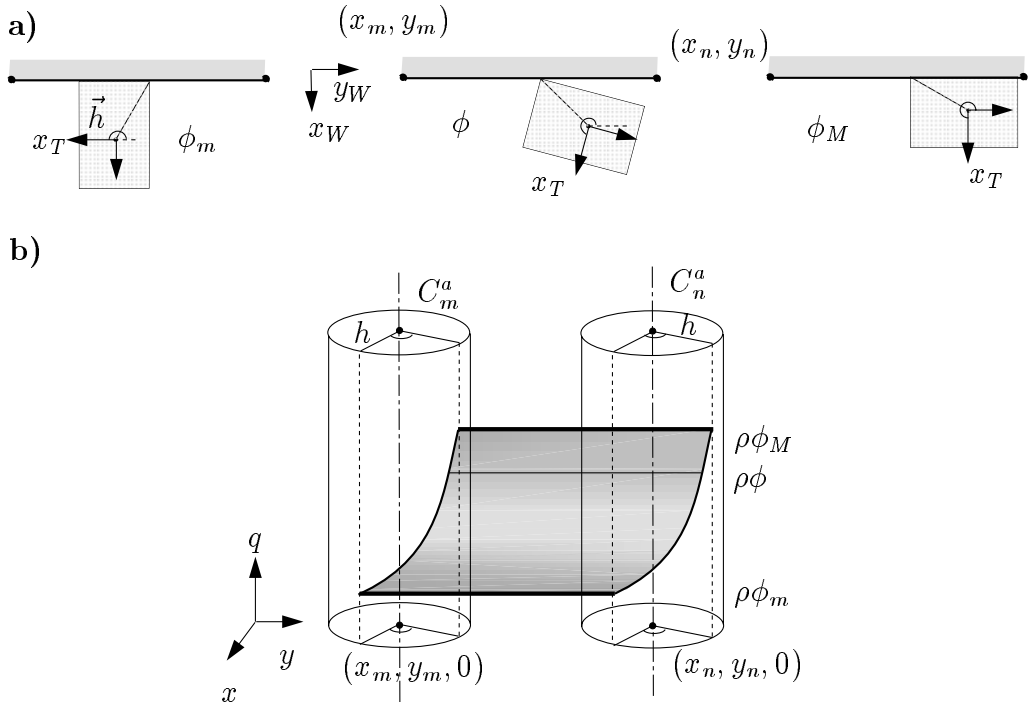

Figure 2.2: *Representation of a type-B basic contact in physical space (a) and in configuration space (b).*

Therefore, for a basic contact i the straight line that contains the ruling segment of the $\mathcal{C}$-face for a given orientation ϕ is:

$$\begin{aligned} x\cos\psi_{Wi} + y\sin\psi_{Wi} &= D_i \\ q &= \rho\phi \end{aligned} \tag{2.6}$$

D_i being defined by equation (2.4) or (2.5), depending on the type of basic contact.

The contact configurations can also be represented in the translational configuration space, as shown below.

Definition 7: The *supporting circumference* c_m^a is the projection on the xy-plane of the supporting cylinder C_m^a, i.e. it is the circumference of radius h_a and center (x_m, y_m).

Proposition 2: *The $\mathcal{C}'$-space contains the same information as the $\mathcal{C}$-space.*

Proof: The projection of each helix representing the extremes of the ruling segments of a $\mathcal{C}$-face is an arc over a supporting circumference. This projection can be parametrized taking the projection of the point corresponding to $q = 0$ as the reference of orientation on the supporting circumference. The angle between the radius to any point of the arc and this reference, expresses the orientation ϕ of the corresponding point in the $\mathcal{C}$-space. Therefore, the projection of any ruling segment contains the information of its orientation in any of its extremes, which are points of an arc over the supporting circumference. $\diamond$

Definition 8: The *$\mathcal{C}'$-face* $\mathcal{F}_i'$ corresponding to a given basic contact i is the parameterized projection of $\mathcal{F}_i$ into the xy-plane.

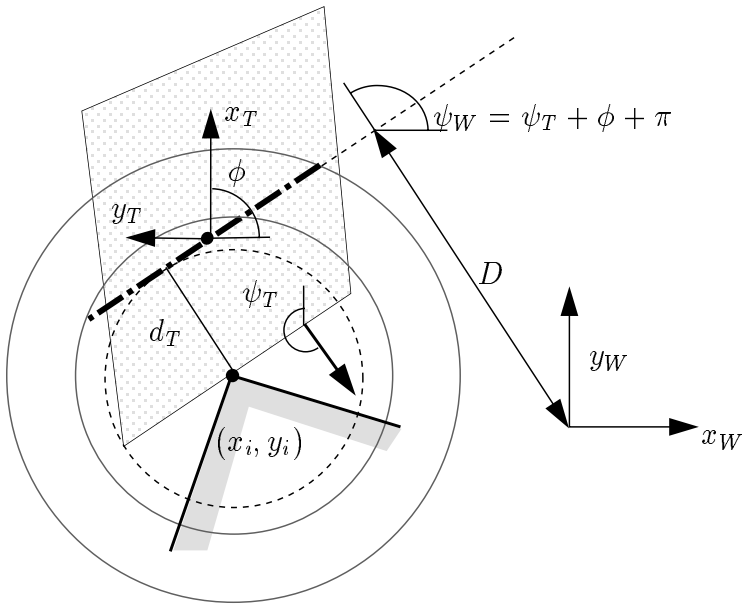

Figure 2.3: *Distance D to the origin of $\{W\}$ of the projection on the xy-plane of the line that supports the ruling segment for a given orientation corresponding to a type-A basic contact.*

Definition 9: The *$\mathcal{C}'$-segment* $f'_i(\phi_o)$ is the projection into the xy-plane of the ruling segment of $\mathcal{F}_i$ corresponding to the orientation ϕ_o. $f'_i(\phi_o)$ has its extremes on the two supporting circumferences associated to the basic contact.

Proposition 3: *$\mathcal{F}'_i$ is the region swept by $f'_i(\phi)$ when its extremes move along the two arcs over the supporting circumferences, when ϕ varies within the set of contact orientations R^i_ϕ:*

$$\mathcal{F}'_i = \bigcup_{\phi \in R^i_\phi} f'_i(\phi) \tag{2.7}$$

Corollary 3.1: For a type-A basic contact between the vertex M of the fixed object and the edge of the manipulated object limited by the vertices A and B, the supporting circumferences are c^a_m and c^b_m, and the ruling segments are tangent to a circumference concentrical with the supporting ones, and with radius equal to the distance from $\{O_\mathcal{A}\}$ to the line containing the contact edge. For type-A basic contacts the orientations will be measured in this latter circumference, where the reference orientation will be attached. Figure 2.5a shows the $\mathcal{C}$-face and the $\mathcal{C}'$-face corresponding to the type-A basic contact shown in Figure 2.1a.

Corollary 3.2: For a type-B basic contact between the vertex A of the manipulated object and the edge of the fixed object limited by the vertices M and N, the supporting circumferences are c^a_m and c^a_n, and the segments are parallel. Figure 2.5b shows the $\mathcal{C}$-face and the $\mathcal{C}'$-face corresponding to the type-B basic contact shown in Figure 2.2a.

As an example Figures 2.6a and 2.6b show the $\mathcal{C}'$-faces corresponding to a type-B and a type-A basic contacts, respectively, of the peg-into-hole assembly task.

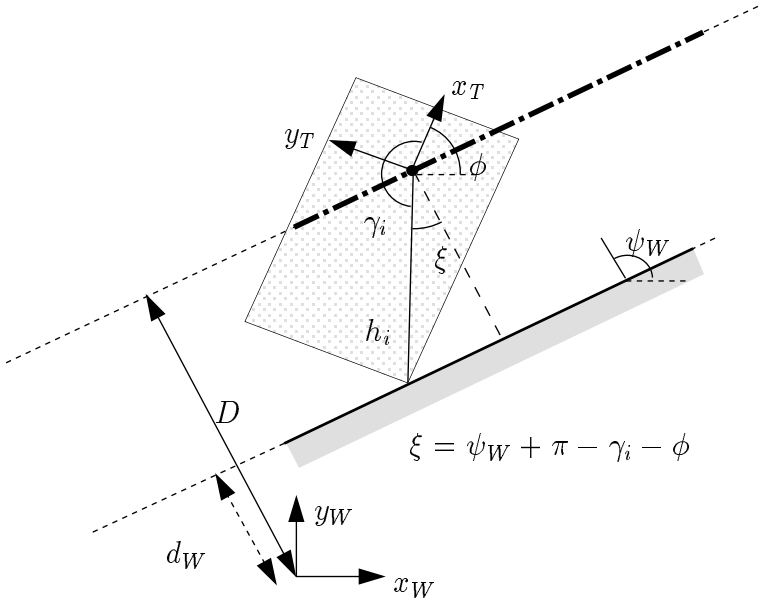

Figure 2.4: *Distance D to the origin of $\{W\}$ of the projection on the xy-plane of the line that supports the ruling segment for a given orientation corresponding to a type-B basic contact.*

2.2.2 Set of contact orientations

For a contact situation involving one basic contact i, the set of contact orientations R^i_ϕ is computed as follows. Let ψ^{sta}_W and ψ^{mob}_T be the orientations of the external normals to an edge of the static object measured in $\{W\}$, and to an edge of the manipulated object measured in $\{T\}$, respectively. The condition

$$\psi^{sta}_W = \phi + \psi^{mob}_T + \pi \tag{2.8}$$

imposes the parallelism between both edges. The orientations ϕ^i_m and ϕ^i_M for which the adjacent edges of the contact vertex are parallel to the contact edge are evaluated using equation (2.8). These orientations are the limits of R^i_ϕ:

$$R^i_\phi = \{\phi \mid \phi \in [\phi^i_m, \phi^i_M]\} \tag{2.9}$$

2.3 Two basic contacts situations

2.3.1 Representation in configuration space

Definition 10: The $\mathcal{C}$-edge $\mathcal{E}_{ij}$ corresponding to a contact situation involving two basic contacts i and j is the set of configurations in the $\mathcal{C}$-space for which the contact situation takes place, only considering the constraints imposed by the edges and vertices involved in any of the contacts.

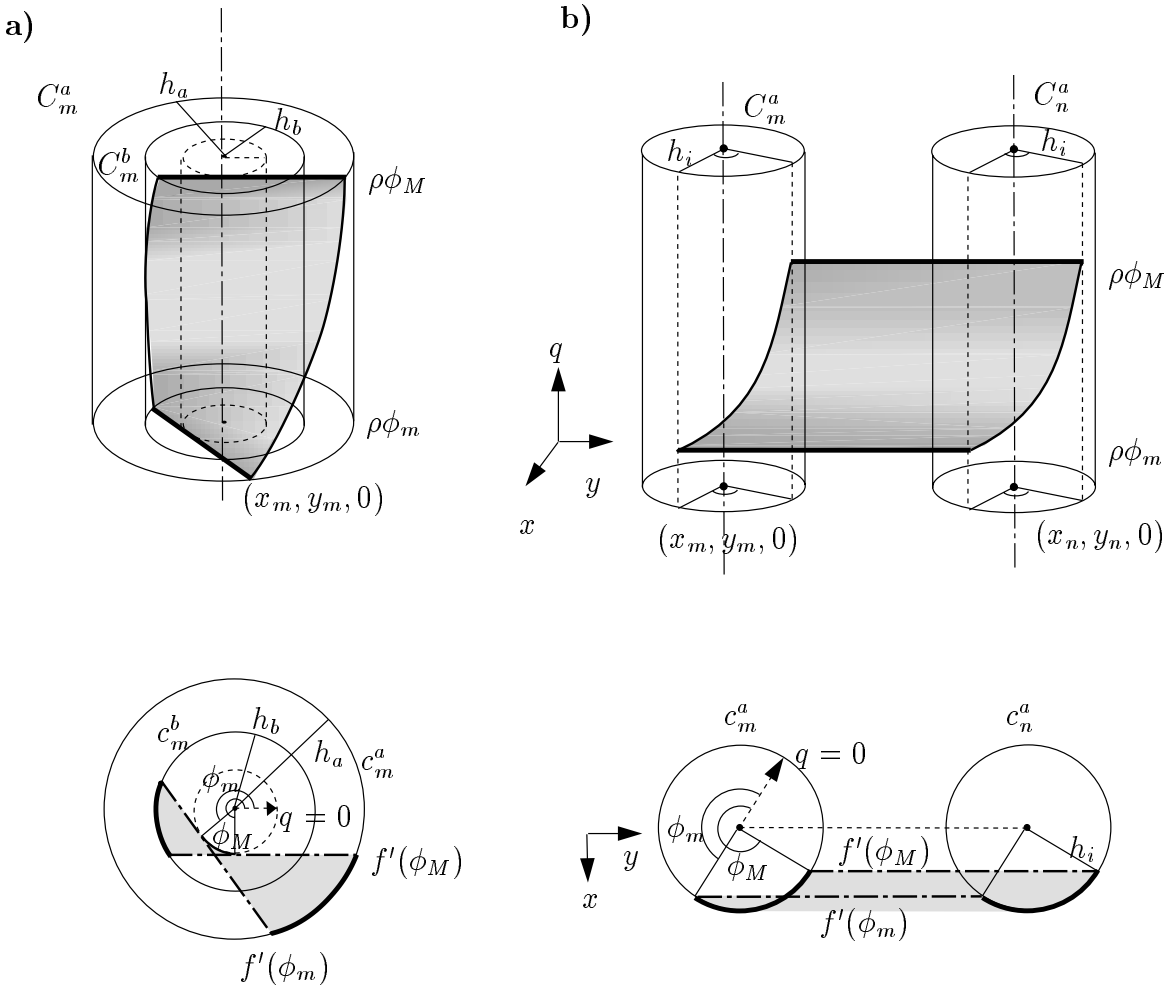

Figure 2.5: *Representation of a type-A and a type-B basic contacts in $\mathcal{C}$-space and in $\mathcal{C}'$-space.*

Definition 11: The *$\mathcal{C}'$-edge* $\mathcal{E}'_{ij}$ corresponding to a given contact situation involving two basic contacts i and j is the parameterized projection of $\mathcal{E}_{ij}$ into the xy-plane:

$$\mathcal{E}'_{ij} = \bigcup_{\phi \in R_\phi^{ij}} f'_i(\phi) \cap f'_j(\phi) \tag{2.10}$$

Proposition 4: *$\mathcal{E}'_{ij}$ is the arc of a curve $\mathcal{L}'_{ij}(\phi)$ for $\phi \in R_\phi^{ij}$. If $\sin(\psi_{Wj} - \psi_{Wi}) \neq 0$ then $\mathcal{L}'_{ij}(\phi)$ is:*

$$\begin{aligned} x &= \frac{D_i \sin(\psi_{Wj}) - D_j \sin(\psi_{Wi})}{\sin(\psi_{Wj} - \psi_{Wi})} \\ y &= -\frac{D_i \cos(\psi_{Wj}) - D_j \cos(\psi_{Wi})}{\sin(\psi_{Wj} - \psi_{Wi})} \\ q &= \rho\phi \end{aligned} \tag{2.11}$$

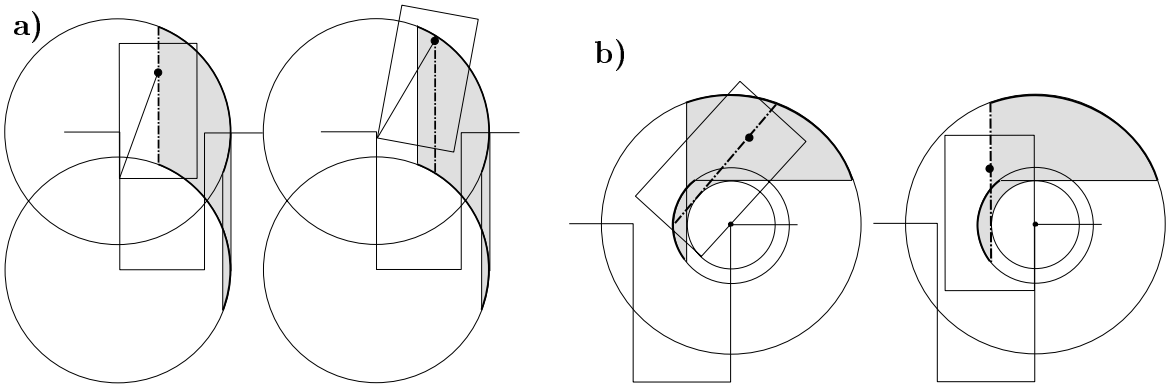

Figure 2.6: *Examples of $\mathcal{C}'$-faces for a type-B (a) and type-A (b) basic contacts of the peg-into-hole assembly task.*

Otherwise $\mathcal{L}'_{ij}(\phi)$ is the straight line:

$$\begin{aligned} x\cos(\psi_{Wi}) + y\sin(\psi_{Wi}) &= D_i \\ q &= \rho\phi \end{aligned} \tag{2.12}$$

defined for the orientation that satisfies $D_i = D_j$.

Corollary 4: For two type-1 basic contacts, equation (2.11) describes an ellipse whose axes are over the bisecting lines of the angles defined by the directions of the contact edges, being their length dependent on the values of h and γ describing the contact vertices of the manipulated object.

Proof: Each point of $\mathcal{L}'_{ij}(\phi)$ lies at the intersection of the lines containing the $\mathcal{C}'$-segments corresponding to a different value of the orientation, which is described by the following system of equations:

$$\begin{aligned} x\cos\psi_{Wi} + y\sin\psi_{Wi} &= D_i \\ x\cos\psi_{Wj} + y\sin\psi_{Wj} &= D_j \end{aligned} \tag{2.13}$$

If $\sin(\psi_{Wj} - \psi_{Wi}) \neq 0$, solving for x and y it leads to equation (2.11). Otherwise the solution is the straight line described by equation (2.12). ◇

2.3.2 Set of contact orientations

Definition 12: The *domain* D^{ij}_{ϕ} of contact orientations for a contact situation involving two basic contacts i and j is the following set of orientations:

$$D^{ij}_{\phi} = R^i_{\phi} \cap R^j_{\phi} = \{\phi \mid \phi \in [\phi^i_m, \phi^i_M] \cap [\phi^j_m, \phi^j_M]\} \tag{2.14}$$

i.e. the contact situation can only occur for orientations for which each of the involved basic contacts can simultaneously occur.

The set of contact orientations R_ϕ^{ij} is a unique orientation when $\sin(\psi_{Wj} - \psi_{Wi}) = 0$. This orientation satisfies the following condition:

$$|D_i| = |D_j| \tag{2.15}$$

Which can be rewritten as

$$a\cos\phi + b\sin\phi = c \tag{2.16}$$

The value of R_ϕ^{ij} is the solution of (2.16) that satisfies $\phi \in D_\phi^{ij}$:

$$\phi = 2\arctan\left(\frac{-b \pm \sqrt{b^2 + a^2 - c^2}}{-a - c}\right) \tag{2.17}$$

The values of a,b and c depend on the type of the involved basic contacts:

- For two type-A basic contacts:

$$\begin{aligned} a &= -x_i\cos\psi_{Ti} - y_i\sin\psi_{Ti} + s\ x_j\cos\psi_{Tj} + s\ y_j\sin\psi_{Tj} \\ b &= x_i\sin\psi_{Ti} - y_i\cos\psi_{Ti} - s\ x_j\sin\psi_{Tj} + s\ y_j\cos\psi_{Tj} \\ c &= s\ d_{Tj} - d_{Ti} \end{aligned} \tag{2.18}$$

  where $s = 1$ if $\psi_{Ti} = \psi_{Tj}$ and $s = -1$ if $\psi_{Ti} = \psi_{Tj} + \pi$.

- For two type-B basic contacts:

$$\begin{aligned} a &= h_i\cos(\gamma_i - \psi_{Wi}) - s\ h_j\cos(\gamma_j - \psi_{Wj}) \\ b &= h_j\sin(\gamma_j - \psi_{Wj}) - s\ h_i\sin(\gamma_i - \psi_{Wi}) \\ c &= s\ d_{Wj} - d_{Wi} \end{aligned} \tag{2.19}$$

  where $s = 1$ if $\psi_{Wi} = \psi_{Wj}$ and $s = -1$ if $\psi_{Wi} = \psi_{Wj} + \pi$.

- For one of each type:

$$\begin{aligned} a &= -h_i\cos(\gamma_i - \psi_{Wi}) + s\ x_j\cos\psi_{Tj} + s\ y_j\sin\psi_{Tj} \\ b &= h_i\sin(\gamma_i - \psi_{Wi}) - s\ x_j\sin\psi_{Tj} + s\ y_j\cos\psi_{Tj} \\ c &= s\ d_{Tj} - d_{Wi} \end{aligned} \tag{2.20}$$

  where a set of solutions is found for $s = 1$ and another one for $s = -1$.

When $\sin(\psi_{Wj} - \psi_{Wi}) \neq 0$, R_ϕ^{ij} is constrained by the orientation of the edges involved in the contact and/or by their finite length. When the orientation constrains the limit of R_ϕ^{ij}, this limit is determined by the corresponding limit of D_ϕ^{ij}. When the constraint is the finite length of an edge the limit is determined by the orientation where an extreme of the corresponding $\mathcal{C}'$-segment f_i' belongs to the other $\mathcal{C}'$-segment f_j', since $\mathcal{E}_{ij}'$ is the intersection of f_i' and f_j'. This orientation is computed as follows.

Let us define:

- (v_{xj}, v_{yj}): an extreme of f_j', i.e. it is a point of one of the supporting circumferences c of contact j:

$$\begin{aligned} v_{xj} &= x_j + h_j\cos(\pi + \phi + \gamma_j) \\ v_{yj} &= y_j + h_j\sin(\pi + \phi + \gamma_j) \end{aligned}$$

- V_j: the distance to the origin of $\{W\}$ of a line parallel to the edge of contact i, and passing through the point (v_{xj}, v_{yj}).

$$V_j = v_{xj} \cos \psi_{Wi} + v_{yj} \sin \psi_{Wi} \tag{2.21}$$

  where ψ_W depends on ϕ for type-A basic contacts.

The orientation satisfying:

$$V_j = D_i \tag{2.22}$$

is the orientation for which the line containing f_i' also contains an extreme of f_j'. If this extreme belongs to f_i' then the orientation is a limit of R_ϕ^{ij}. Condition (2.22) can be rewritten as:

$$a \cos \phi + b \sin \phi = c \tag{2.23}$$

The values of a,b and c depend on the type of the involved basic contacts:

- If i is a type-A basic contact:

$$\begin{aligned} a &= (x_j - x_i) \cos \psi_{Ti} + (y_j - y_i) \sin \psi_{Ti} \\ b &= -(x_j - x_i) \sin \psi_{Ti} + (y_j - y_i) \cos \psi_{Ti} \\ c &= h_j \cos(\psi_{Ti} - \gamma_j) - d_{Ti} \end{aligned} \tag{2.24}$$

- If i is a type-B basic contact:

$$\begin{aligned} a &= h_j \cos(\gamma_j - \psi_{Wi}) - h_i \cos(\gamma_i - \psi_{Wi}) \\ b &= h_i \sin(\gamma_i - \psi_{Wi}) - h_j \sin(\gamma_j - \psi_{Wi}) \\ c &= x_j \cos \psi_{Wi} + y_j \sin \psi_{Wi} - d_{Wi} \end{aligned} \tag{2.25}$$

The solution of (2.23) is (2.17).

As an example, Figures 2.7a and 2.7b show two type-B basic contacts and Figures 2.7c and 2.7d the curve $\mathcal{L}_{ij}'$, which is an ellipse, and the $\mathcal{C}'$-edge $\mathcal{E}_{ij}'$ corresponding to the contact situation involving both contacts. The inferior limit of R_ϕ^{ij} is constrained by the finite length ot the contact edge of the basic contact of Figure 2.7a, and is shown in Figure 2.7c. The superior limit of R_ϕ^{ij} is constrained by the orientation of the edges involved in the contact and is shown in Figure 2.7d.

Figure 2.8 and 2.9 show the same as Figure 2.7 but for two type-A basic contacts and for one of each type, respectively.

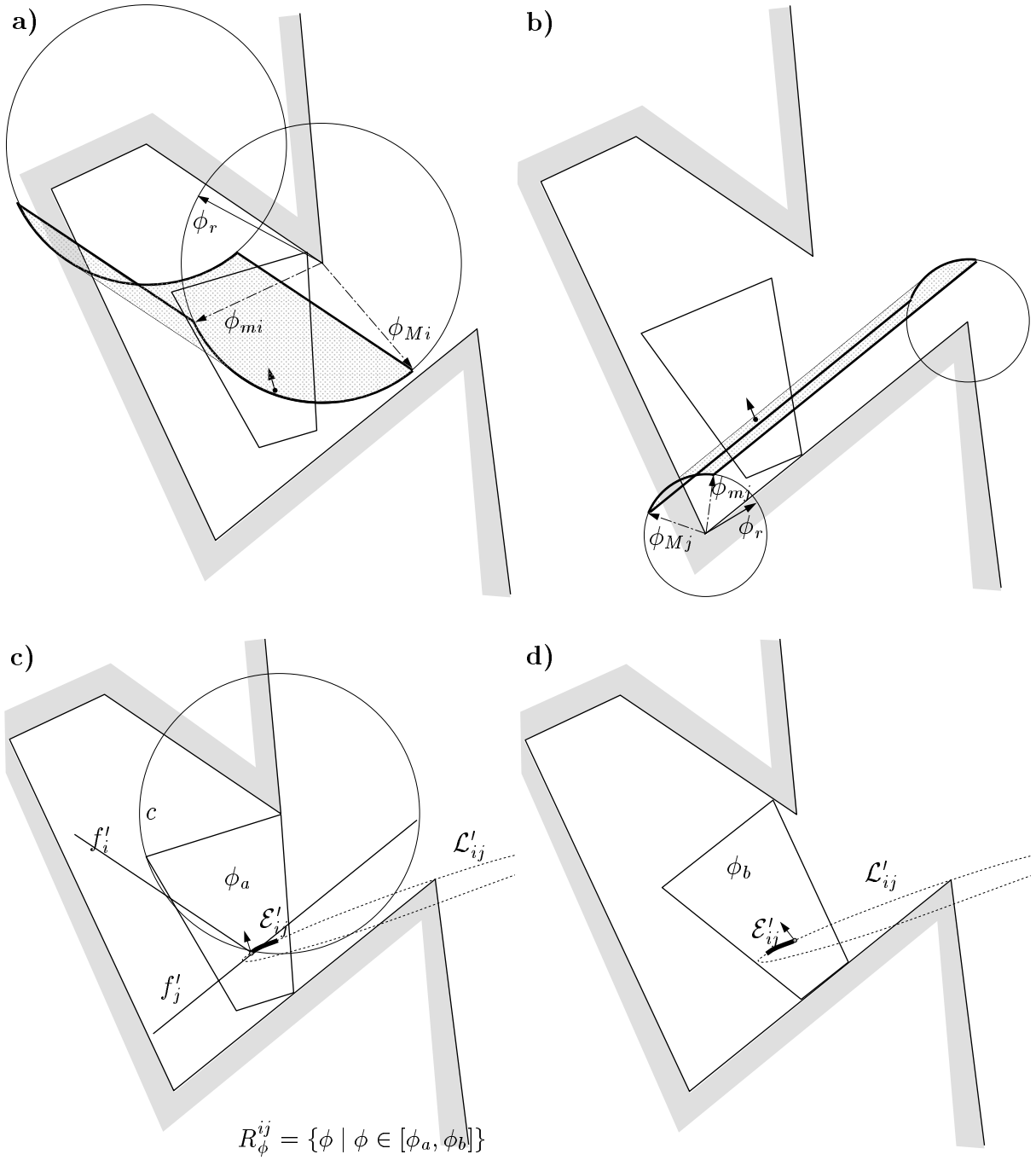

Figure 2.7: *$\mathcal{C}'$-faces of two type-B basic contacts (a and b) and the corresponding $\mathcal{C}'$-edge $\mathcal{E}'_{ij}$ (c and d). $\mathcal{E}'_{ij}$ is a segment of the curve $\mathcal{L}'_{ij}$ for the set of contact orientations $R_\phi^{ij} = \{\phi \mid \phi \in [\phi_a, \phi_b]\}$. The orientation ϕ_a is determined by the finite length of a contact edge (c). The orientation ϕ_b is determined by an orientation constraint (d).*

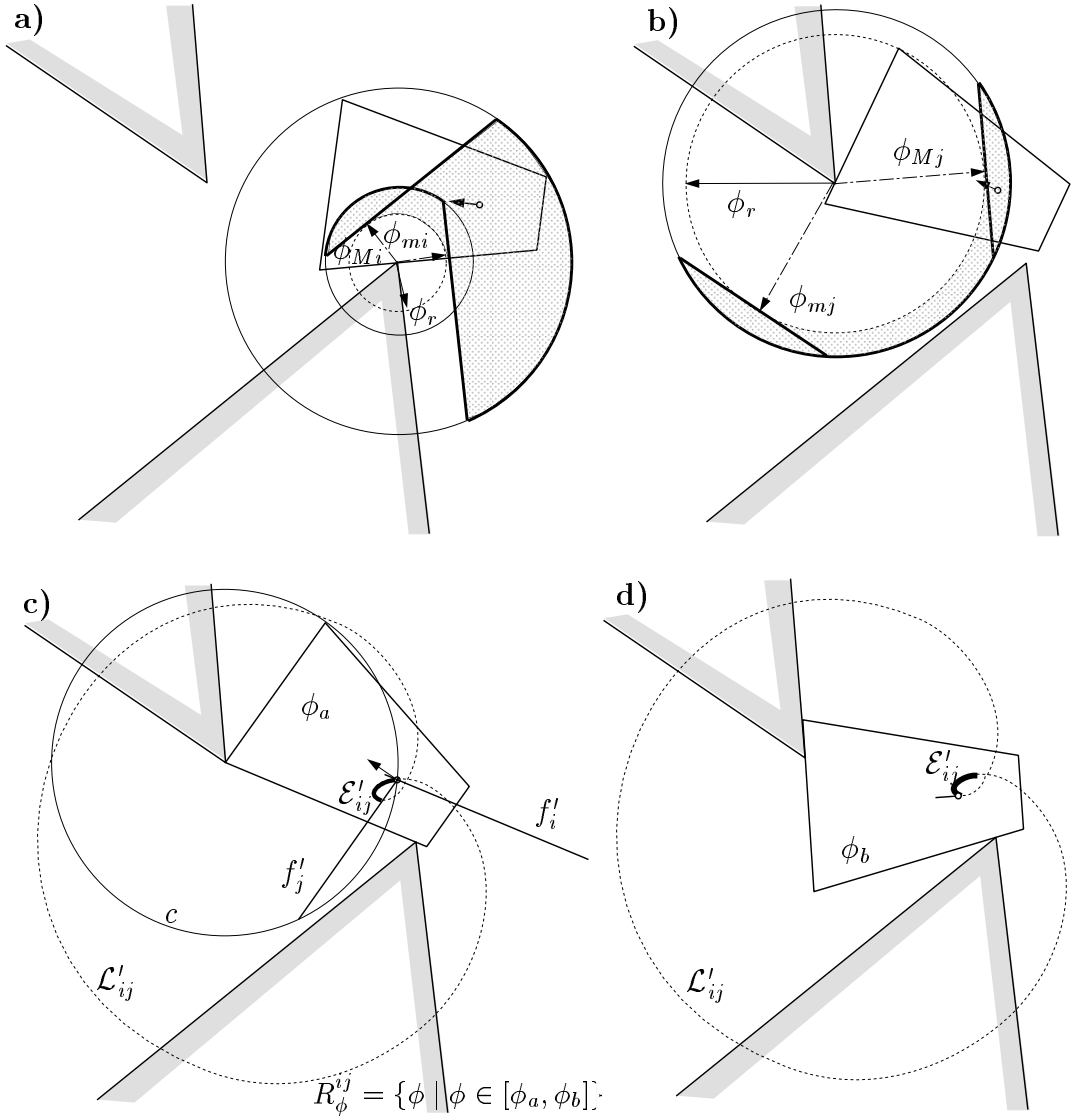

Figure 2.8: *$\mathcal{C}'$-faces of two type-A basic contacts (a and b) and the corresponding $\mathcal{C}'$-edge $\mathcal{E}'_{ij}$ (c and d). $\mathcal{E}'_{ij}$ is a segment of the curve $\mathcal{L}'_{ij}$ for the set of contact orientations $R^{ij}_\phi = \{\phi \mid \phi \in [\phi_a, \phi_b]\}$. The orientation ϕ_a is determined by the finite length of a contact edge (c). The orientation ϕ_b is determined by an orientation constraint (d).*

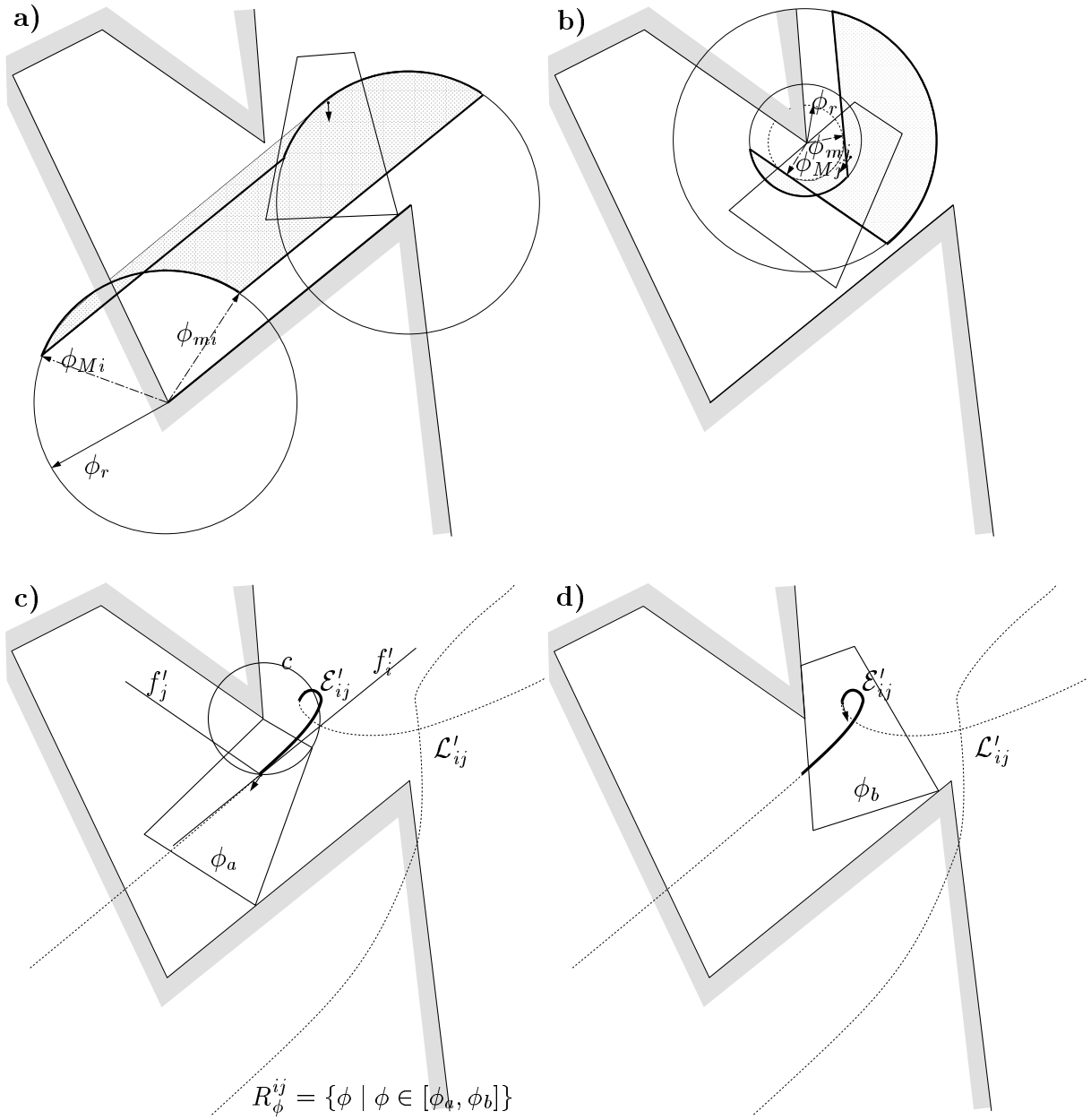

Figure 2.9: *$\mathcal{C}'$-faces of a type-A (a) and a type-B (b) basic contact, and the corresponding $\mathcal{C}'$-edge $\mathcal{E}'_{ij}$ (c and d). $\mathcal{E}'_{ij}$ is a segment of the curve $\mathcal{L}'_{ij}$ for the set of contact orientations $R^{ij}_\phi = \{\phi \mid \phi \in [\phi_a, \phi_b]\}$. The orientation ϕ_a is determined by the finite length of a contact edge (c). The orientation ϕ_b is determined by an orientation constraint (d).*

2.4 Three and more basic contacts situations

2.4.1 Representation in configuration space

Since planar movements have three degrees of freedom, the contact situations involving three non-redundant basic contacts take place only at a given configuration. If there are $n > 3$ basic contacts, $n - 3$ will be redundant.

Definition 13: The $\mathcal{C}$-vertex $\mathcal{V}_{ijk}$ corresponding to a contact situation involving three basic contacts i, j and k is the configuration in the $\mathcal{C}$-space for which the contact situation takes place.

If one of the contacts is redundant, e.g. when the three corresponding $\mathcal{C}$-edges are parallel segments that take place at a unique orientation, then the three basic contact can take place at all the configurations of a segment where the three $\mathcal{C}$-edges intersect. In this case the two extremes of this segment are considered as $\mathcal{C}$-vertices.

Definition 14: The $\mathcal{C}'$-vertex $\mathcal{V}'_{ijk}$ is the representation of $\mathcal{V}_{ijk}$ in the $\mathcal{C}'$-space.

2.4.2 Set of contact orientations

Proposition 5: *The orientation where a contact situation involving three basic contacts i, j and k can occur satisfies the following condition:*

$$D_i \sin(\psi_{Wj} - \psi_{Wk}) + D_j \sin(\psi_{Wk} - \psi_{Wi}) + D_k \sin(\psi_{Wi} - \psi_{Wj}) = 0 \tag{2.26}$$

if $\sin(\psi_{Wj} - \psi_{Wk}) \neq 0$, $\sin(\psi_{Wk} - \psi_{Wi}) \neq 0$ *and* $\sin(\psi_{Wi} - \psi_{Wj}) \neq 0$. *Otherwise it is the unique orientation where one of the contact situation involving two basic contacts occurs.*

Proof: Let (2.27) express the coordinates of a point (x, y) of the $\mathcal{C}'$-edge $\mathcal{E}'_{ij}$ for a given orientation, and let (2.28) be the equation of a line l_k containing the ruling segment of contact k for that orientation. Then, if $(x, y) \in l_k$, this point can be the $\mathcal{C}'$-vertex:

$$\begin{aligned} x &= \frac{D_i \sin(\psi_{Wj}) - D_j \sin(\psi_{Wi})}{\sin(\psi_{Wj} - \psi_{Wi})} \\ y &= -\frac{D_i \cos(\psi_{Wj}) - D_j \cos(\psi_{Wi})}{\sin(\psi_{Wj} - \psi_{Wi})} \end{aligned} \tag{2.27}$$

$$x \cos(\psi_{Wk}) + y \sin(\psi_{Wk}) = D_k \tag{2.28}$$

Substituting (2.27) in (2.28), it leads to (2.26). ◇

Corollary 5.1: When the three basic contacts are of the same type, equation (2.26) becomes:

$$a \cos\phi + b \sin\phi = c \tag{2.29}$$

The values of a,b and c depend on the type of the involved basic contacts:

- For three type-A basic contacts:

$$\begin{aligned} a &= (x_i \cos\psi_{Ti} + y_i \sin\psi_{Ti}) \sin(\psi_{Wj} - \psi_{Wk}) + \\ &\quad (x_j \cos\psi_{Tj} + y_j \sin\psi_{Tj})) \sin(\psi_{Wk} - \psi_{Wi}) + \\ &\quad (x_k \cos\psi_{Tk} + y_k \sin\psi_{Tk}) \sin(\psi_{Wi} - \psi_{Wj}) \\ b &= (-x_i \sin\psi_{Ti} + y_i \cos\psi_{Ti}) \sin(\psi_{Wj} - \psi_{Wk}) + \\ &\quad (-x_j \sin\psi_{Tj} + y_j \cos\psi_{Tj})) \sin(\psi_{Wk} - \psi_{Wi}) + \\ &\quad (-x_k \sin\psi_{Tk} + y_k \cos\psi_{Tk}) \sin(\psi_{Wi} - \psi_{Wj}) \\ c &= d_{Ti} \sin(\psi_{Tj} - \psi_{Tk}) + d_{Tj} \sin(\psi_{Tk} - \psi_{Ti}) + d_{Tk} \sin(\psi_{Ti} - \psi_{Tj}) \end{aligned} \quad (2.30)$$

- For three type-B basic contacts:

$$\begin{aligned} a &= h_i \cos(\gamma_i - \psi_{Wi}) \sin(\psi_{Wj} - \psi_{Wk}) + \\ &\quad h_j \cos(\gamma_j - \psi_{Wj}) \sin(\psi_{Wk} - \psi_{Wi}) + \\ &\quad h_k \cos(\gamma_k - \psi_{Wk}) \sin(\psi_{Wi} - \psi_{Wj}) \\ b &= -h_i \sin(\gamma_i - \psi_{Wi}) \sin(\psi_{Wj} - \psi_{Wk}) + \\ &\quad -h_j \sin(\gamma_j - \psi_{Wj}) \sin(\psi_{Wk} - \psi_{Wi}) + \\ &\quad -h_k \sin(\gamma_k - \psi_{Wk}) \sin(\psi_{Wi} - \psi_{Wj}) \\ c &= d_{Wi} \sin(\psi_{Wj} - \psi_{Wk}) + d_{Wj} \sin(\psi_{Wk} - \psi_{Wi}) + d_{Wk} \sin(\psi_{Wi} - \psi_{Wj}) \end{aligned} \quad (2.31)$$

The solution of (2.29) is (2.17).

Corollary 5.2: When the contacts are of different type, equation (2.26) becomes:

$$a \sin^2\phi + b \cos^2\phi + c \sin\phi \cos\phi + d \sin\phi + e \cos\phi + f = 0 \quad (2.32)$$

The values of a,b,c,d and e depend on the type of the involved basic contacts:

- When i and j are type-B and k is type-A:

$$\begin{aligned} a &= h_i \cos(\gamma_i - \psi_{Wi}) \sin(\psi_{Tk} - \psi_{Wj}) - h_j \cos(\gamma_j - \psi_{Wj}) \sin(\psi_{Tk} - \psi_{Wi}) \\ b &= -h_i \cos(\gamma_i - \psi_{Wi}) \sin(\psi_{Tk} - \psi_{Wj}) - h_j \cos(\gamma_j - \psi_{Wj}) \sin(\psi_{Tk} - \psi_{Wi}) \\ c &= -h_i \cos(\gamma_i + \psi_k - \psi_j - \psi_i) + h_j \cos(\gamma_j + \psi_k - \psi_j - \psi_i) \\ d &= d_{Wi} \cos(\psi_{Tk} - \psi_{Wj}) - d_{Wj} \cos(\psi_{Tk} - \psi_{Wi}) + (x_k \sin\psi_{Tk} - y_k \cos\psi_{Tk}) \sin(\psi_{Ti} - \psi_{Wj}) \\ e &= d_{Wi} \sin(\psi_{Tk} - \psi_{Wj}) - d_{Wj} \sin(\psi_{Tk} - \psi_{Wi}) + (-x_k \cos\psi_{Tk} - y_k \sin\psi_{Tk}) \sin(\psi_{Ti} - \psi_{Wj}) \\ f &= d_{Tk} \sin(\psi_{Wj} - \psi_{Wi}) \end{aligned} \quad (2.33)$$

- When i is type-B and j and k are type-A:

$$\begin{aligned} a &= -(x_j \sin\psi_{Tj} - y_j \cos\psi_{Tj}) \cos(\psi_{Tk} - \psi_{Wi}) + (x_k \sin\psi_{Tk} - y_k \cos\psi_{Tk}) \cos(\psi_{Tj} - \psi_{Wi}) \\ b &= (x_j \cos\psi_{Tj} + y_j \sin\psi_{Tj}) \sin(\psi_{Tk} - \psi_{Wi}) + -(x_k \cos\psi_{Tk} + y_k \sin\psi_{Tk}) \sin(\psi_{Tj} - \psi_{Wi}) \\ c &= x_j \cos(\psi_{Tj} + \psi_{Tk} - \psi_{Wi}) + y_j \sin(\psi_{Tj} + \psi_{Tk} - \psi_{Wi}) \\ &\quad -x_k \cos(\psi_{Tj} + \psi_{Tk} - \psi_{Wi}) - y_k \sin(\psi_{Tj} + \psi_{Tk} - \psi_{Wi}) \end{aligned}$$

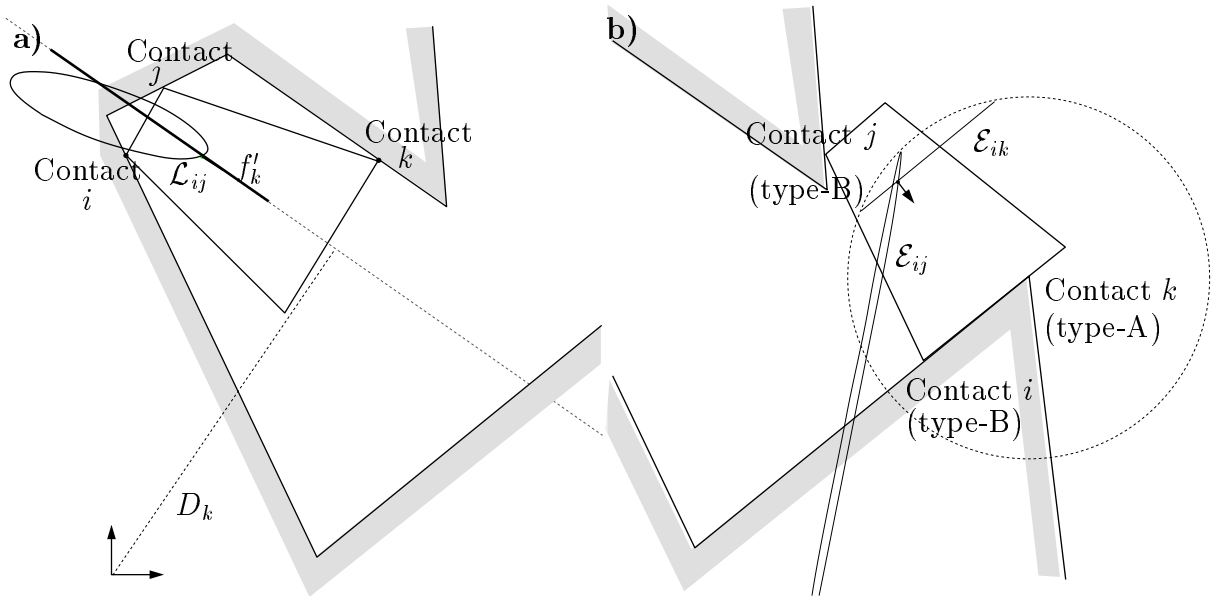

Figure 2.10: *Two $\mathcal{C}'$-vertices corresponding to the contact situation involving a) three type-B basic contacts b) one type-A and two type-B basic contacts.*

$$\begin{aligned} d &= -d_{Tj}\cos(\psi_{Tk}-\psi_{Wi}) + d_{Tk}\cos(\psi_{Tj}-\psi_{Wi}) + h_i\sin(\gamma_i-\psi_{Ti})\sin(\psi_{Tj}-\psi_{Tk}) \\ e &= -d_{Tj}\sin(\psi_{Tk}-\psi_{Wi}) + d_{Tk}\sin(\psi_{Tj}-\psi_{Wi}) - h_i\cos(\gamma_i-\psi_{Ti})\sin(\psi_{Tj}-\psi_{Tk}) \\ f &= d_{Tk}\sin(\psi_{Tj}-\psi_{Tk}) \end{aligned} \tag{2.34}$$

Equation (2.32) is numerically solved.

Corollary 5.3: The obtained point, which is the intersection of the lines containing the $\mathcal{C}'$-segments of the three contacts, will be the $\mathcal{C}'$-vertex if it belongs to the $\mathcal{C}'$-segments.

Figure 2.10a shows a contact situations involving three type-B basic contacts. Figure 2.10b shows a contact situations involving two type-B basic contacts (i and j) and one type-A basic contact (k). In this case, the $\mathcal{C}$-vertex takes place at the unique orientation where the contact situation involving contacts i and k occurs.

2.5 Considering all the geometric constraints

In a given contact situation there can be more constraints than those imposed by the edges and vertices involved in the basic contacts of this situation, either due to concave objects or due to the existence of several static objects. The $\mathcal{C}$-space considering these additional constraints can be built by first generating the $\mathcal{C}$-faces, the $\mathcal{C}$-edges and the $\mathcal{C}$-vertices in this order as described in the previous sections, and then by pruning these sets considering all the constraints. Let $\mathbf{F}_i$ be the subset of $\mathcal{F}_i$ that satisfies all the constraints. If none of the configurations of $\mathcal{F}_i$ satisfies all the constraints, then $\mathbf{F}_i$ does not exist. Let $\mathbf{E}_{ij}$ be defined in a similar way with respect to $\mathcal{E}_{ij}$, and let $\mathbf{V}_{ijk}$ be the C-vertex $\mathcal{V}_{ijk}$ if $\mathcal{V}_{ijk}$ satisfies all the constraints.

2.5.1 Configuration space construction algorithm

In order to find the contact configurations satisfying all the constraints, first the set of $\mathcal{C}$-vertices is prunned by eliminating those $\mathcal{C}$-vertices that correspond to configurations that produce an overlapping of the objects, and then by merging those $\mathcal{C}$-vertices that correspond to the same contact configuration, which corresponds to a contact configuration involving more than three basic contacts.

$\mathcal{C}$-vertex-Pruning()

FOR ALL $\mathcal{C}$-vertices $\mathcal{V}_{ijk}$

IF the edges of the objects do not intersect when the manipulated object is at configuration $\mathcal{V}_{ijk}$ THEN $\mathbf{V}_{ijk} = \mathcal{V}_{ijk}$

Merge the $\mathcal{C}$-vertices that correspond to the same configuration

END

Then, the contact configurations that satisfy all the constraints and belong to a $\mathcal{C}$-edge are identified by the algorithm shown below (Figure 2.11). Let ϕ_m and ϕ_M be two consecutive orientations of $\mathcal{C}$-vertices that involve a given $\mathcal{C}$-edge $\mathcal{E}_{ij}$. Let $\mathcal{V}_{ijk_m}$ be the $\mathcal{C}$-vertex that takes place at orientation ϕ_m, and $\mathcal{F}_{k_m}$ be the $\mathcal{C}$-face of the contact not involved in $\mathcal{E}_{ij}$. Let $\mathcal{V}_{ijk_M}$ and $\mathcal{F}_{k_M}$ be defined in a similar way. Then, the algorithm is a s follows.

$\mathcal{C}$-edge-Pruning()

FOR ALL $\mathcal{C}$-edges $\mathcal{E}_{ij}$:

Find W, the set of $\mathcal{C}$-vertices $\mathbf{V}_{ijk}$ where the $\mathcal{C}$-edge is involved

IF W contains less than two $\mathcal{C}$-certices THEN $\mathbf{E}_{ij}$ does not exist

ELSE

Compute $\vec{n}_{k_m}$ and $\vec{n}_{k_M}$ as the normals to $\mathcal{F}_{k_m}$ and $\mathcal{F}_{k_M}$ at configurations $\mathbf{V}_{ijk_m}$ and $\mathbf{V}_{ijk_M}$, respectively.

Compute $\vec{t}_m$ and $\vec{t}_M$ as the tangent vector to $\mathcal{E}_{ij}$ at orientation ϕ_m and ϕ_M, respectively, such that $\vec{t}_m \cdot \vec{q} > 0$ and $\vec{t}_M \cdot \vec{q} > 0$.

$\mathbf{E}_{ij}$ is composed of the segments of $\mathcal{E}_{ij}$ that satisfy:

- Condition 1: either ϕ_m is a limit of orientation of $\mathcal{E}_{ij}$, or $\vec{t}_m \cdot \vec{n}_{k_m} > 0$.
- Condition 2: either ϕ_M is a limit of orientation of $\mathcal{E}_{ij}$, or $\vec{t}_M \cdot \vec{n}_{k_M} < 0$.

END

Definition 15: A *$\mathcal{C}$-item* is the set of connected configurations of a $\mathcal{C}$-face between two consecutive orientations of the $\mathcal{C}$-vertices of the $\mathcal{C}$-face.

Definition 16: A *$\mathcal{C}$-patch* is the set of $\mathcal{C}$-items that have the same range of orientations.

Let $\mathcal{F}_i$ be the $\mathcal{C}$-face involving a basic contact i. $\mathcal{F}_i$ can be divided in $\mathcal{C}$-patches depending on the orientations of the $\mathcal{C}$-vertices where $\mathcal{F}_i$ is involved. Each $\mathcal{C}$-patch is divided in

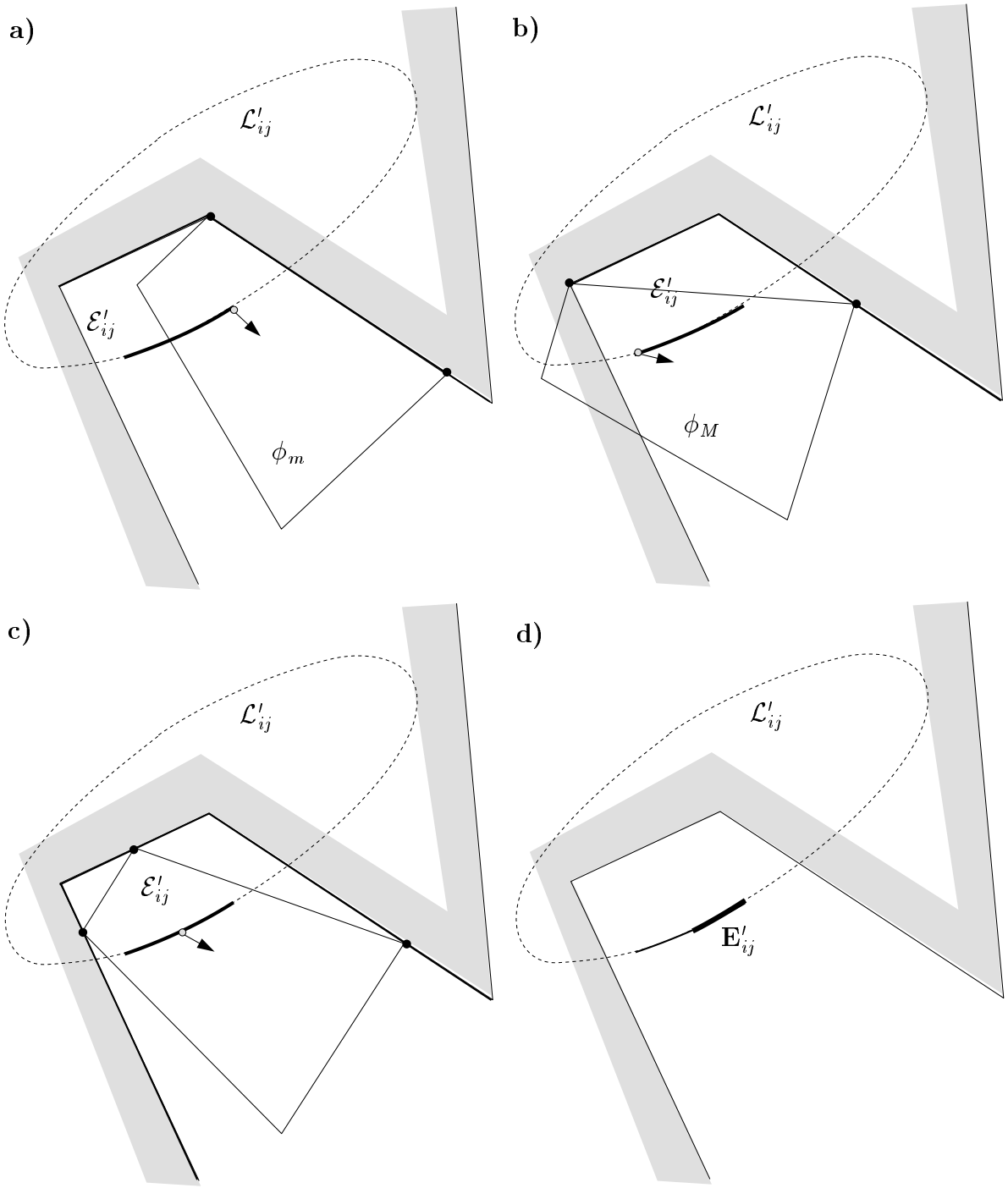

Figure 2.11: *$\mathcal{C}'$-edge: the limits of $\mathcal{E}'_{ij}$ due to the constraints imposed by the edges involved in the basic contacts i and j are ϕ_m (a) and ϕ_M (b). At orientation ϕ_v (c) a $\mathcal{C}'$-vertex occurs involving contacts i, j and k. The orientation ϕ_v divides $\mathcal{E}'_{ij}$ in two segments (d), being $\mathbf{E}'_{ij}$ the prunned $\mathcal{C}'$-edge.*

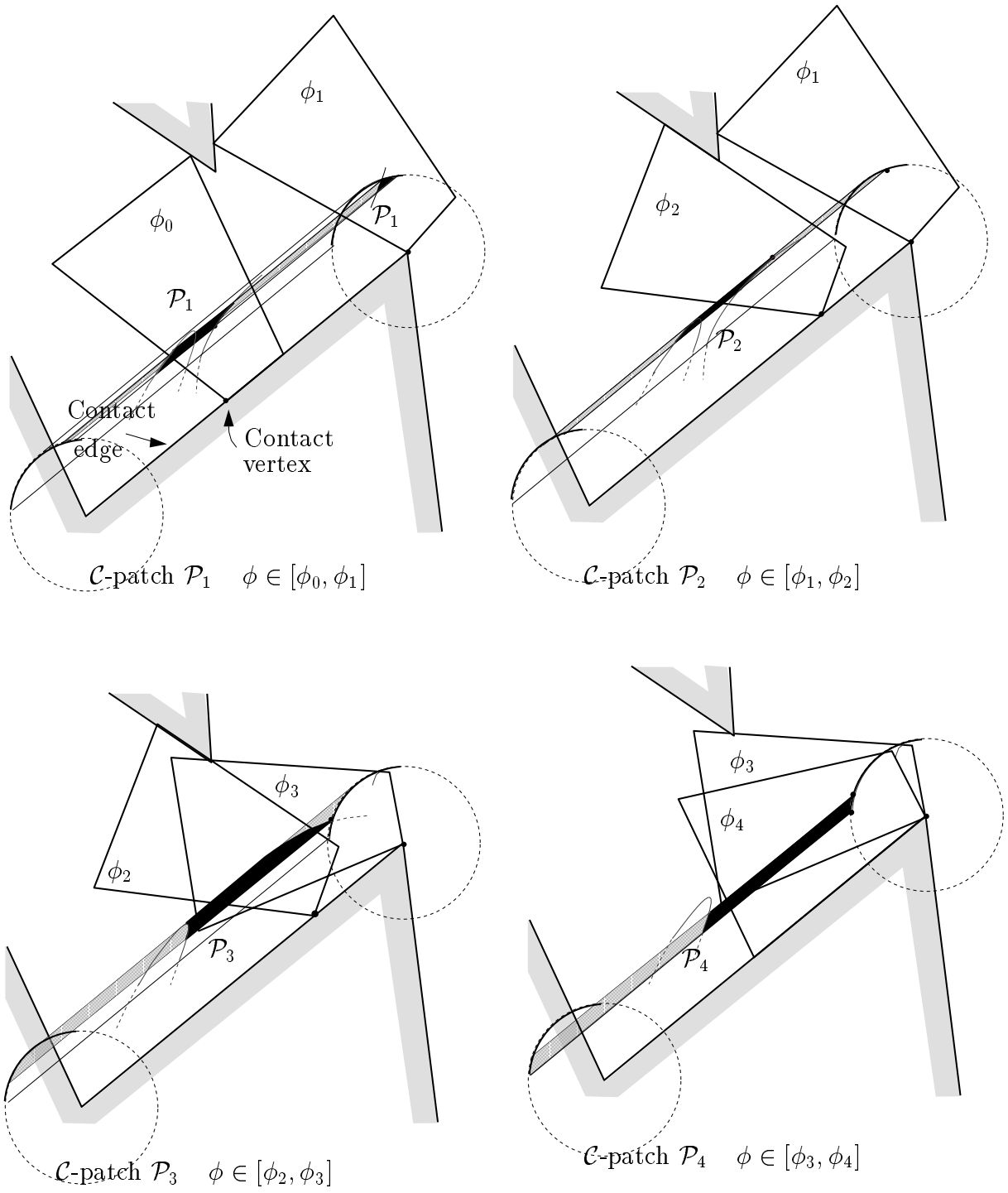

Figure 2.12: *Four $\mathcal{C}$-patches of a $\mathcal{C}$-face. The range of orientations of each $\mathcal{C}$-patch is determined by the orientations ϕ_i of the $\mathcal{C}$-vertices where the $\mathcal{C}$-face is involved. The $\mathcal{C}$-patch $\mathcal{P}_1$ has two $\mathcal{C}$-items.*

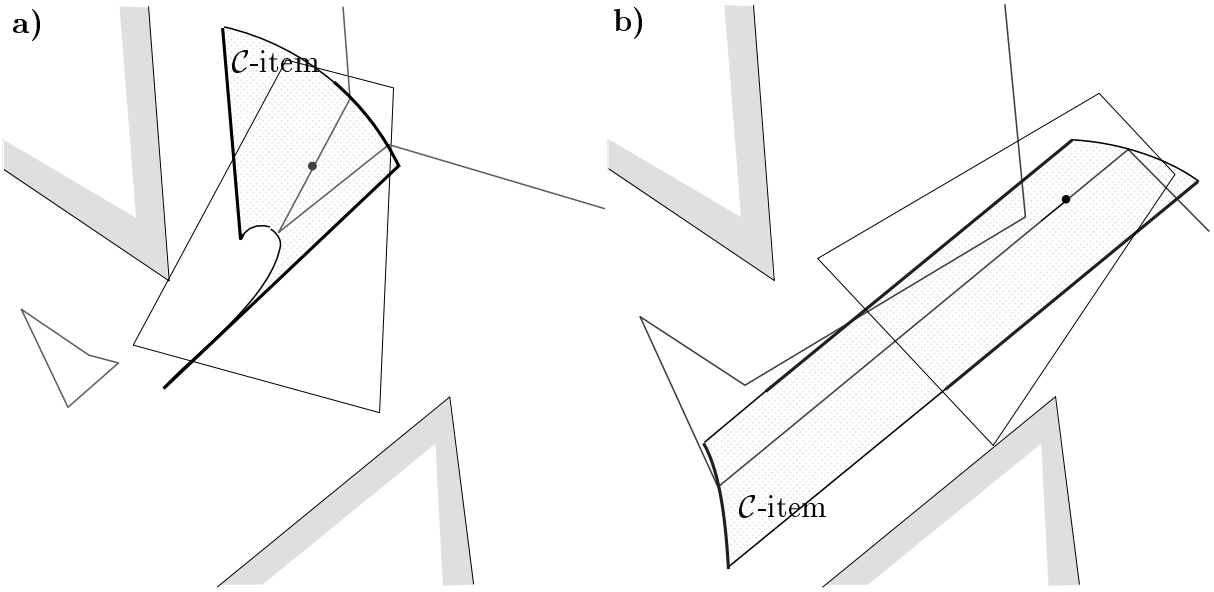

Figure 2.13: *$\mathcal{C}$-item of a type-A (a) and a type-B (b) $\mathcal{C}$-face.*

several $\mathcal{C}$-items depending on the number of $\mathcal{C}$-edges where $\mathcal{F}_i$ is involved in the range of orientations of the $\mathcal{C}$-patch, e.g. if there are only two $\mathcal{C}$-edges, then there is only one $\mathcal{C}$-item. Figure 2.12 shows the four $\mathcal{C}$-patches of a $\mathcal{C}$-face, having one of them two $\mathcal{C}$-items. Figure 2.13 shows two $\mathcal{C}$-items, one corresponding to a type-A basic contact and the other corresponding to a type-B basic contact. The algorithm used to prune the $\mathcal{C}$-faces is shown below. Let ϕ_m and ϕ_M be the minimum and maximum orientations of a $\mathcal{C}$-item of a given $\mathcal{C}$-face $\mathcal{F}_i$. Let $\mathbf{E}_{ij}$ and $\mathbf{E}_{ik}$ be the $\mathcal{C}$-edges that limit the $\mathcal{C}$-item, corresponding to the intersection with the $\mathcal{C}$-faces $\mathcal{F}_j$ and $\mathcal{F}_k$, respectively. Let $\vec{v}$ be defined as $\vec{v} = \mathbf{E}_{ij}(\phi_p) - \mathbf{E}_{ik}(\phi_p)$, with $\phi_p \in [\phi_m, \phi_M]$. Then, the algoritm is as follows:

$\mathcal{C}$-face-Pruning()

FOR ALL $\mathcal{C}$-faces $\mathcal{F}_i$:

Find the $\mathcal{C}$-vertices $\mathbf{V}_{ijk}$ where $\mathcal{F}_i$ is involved

Divide the $\mathcal{C}$-face into $\mathcal{C}$-patches using the orientations of the $\mathcal{C}$-vertices found

FOR ALL the $\mathcal{C}$-patches

Find the $\mathcal{C}$-edges $\mathbf{E}_{ij}$ where the $\mathcal{C}$-face is involved

IF only less than two are found, elimiate the $\mathcal{C}$-patch

ELSE Divide the $\mathcal{C}$-patch into $\mathcal{C}$-items using the $\mathcal{C}$-edges $\mathbf{E}_{ij}$ found

$\mathbf{F}_i$ is composed of the $\mathcal{C}$-items that satisfy:

- Condition 1: the component of $\vec{v}$ along the direction normal to $\mathcal{F}_k$ is positive.
- Condition 2: the component of $\vec{v}$ along the direction normal to $\mathcal{F}_j$ is negative.

END

Finally, the algorithm to construct the $\mathcal{C}$-space is as follows:

$\mathcal{C}$-space-Algorithm()

Compute $\mathcal{F}$, $\mathcal{E}$ and $\mathcal{V}$ for all the contact situations

$\mathcal{C}$-vertex-Pruning()

$\mathcal{C}$-edge-Pruning()

$\mathcal{C}$-face-Pruning()

END

2.5.2 An example

The algorithm to built the $\mathcal{C}$-space has been implemented in C++, using an object oriented methodology, with a Silicon Graphics workstation. Figure 2.14 shows the $\mathcal{C}'$-edges of the $\mathcal{C}'$-space between a convex manipulated object and a concave static object. Figure 2.15 shows the snapshots of the sections for different values of the orientation of the $\mathcal{C}$-space.

2.6 Partition of the configuration space

The basic motion planning problem, i.e. the problem of finding a free path for a robot from an initial configuration to a goal configuration, considering the robot as the only moving object and ignoring its dynamic properties, is a geometric path planning problem. This geometric path planning problem can be solved by the cell decomposition approach. Let the free-space $\mathcal{C}_{free}$ be the subset of the $\mathcal{C}$-space corresponding to non-contact configurations that satisfy all the geometric constraints of the task, and let the contact-space $\mathcal{C}_{contact}$ be the subset of the $\mathcal{C}$-space corresponding to the contact configurations. The cell decomposition approach:

- Decomposes $\mathcal{C}_{free}$ into cells.
- Constructs a graph representing the adjacency between cells.

Then the problem of finding a path between an initial configuration and a goal configuration is done by:

- Searching the graph for a sequence of cells connecting the initial cell (i.e. the cell where the initial configuration belongs to) with the goal cell.
- Searching a path between two configurations of each cell in order to connect the adjacent cells of the sequence (cells are built in such a way that the path between any two configurations of a cell is easily obtained).

Different methods follow the cell decomposition approach, each of them decomposing $\mathcal{C}_{free}$ into different kinds of cells. Nevertheless, they can be classified in two groups:

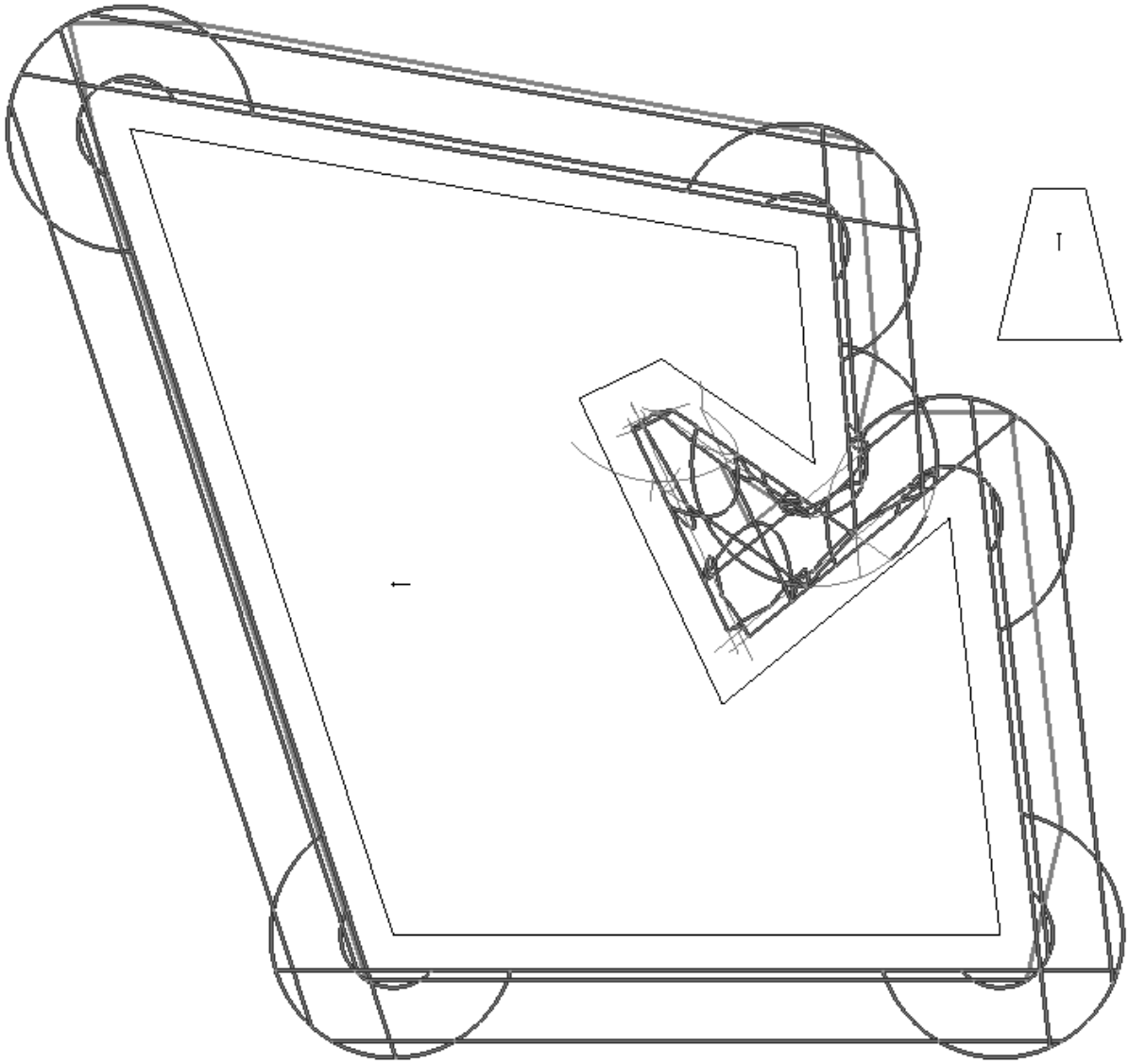

Figure 2.14: *$\mathcal{C}'$-edges of the $\mathcal{C}'$-space between a convex manipulated object and a concave static object.*

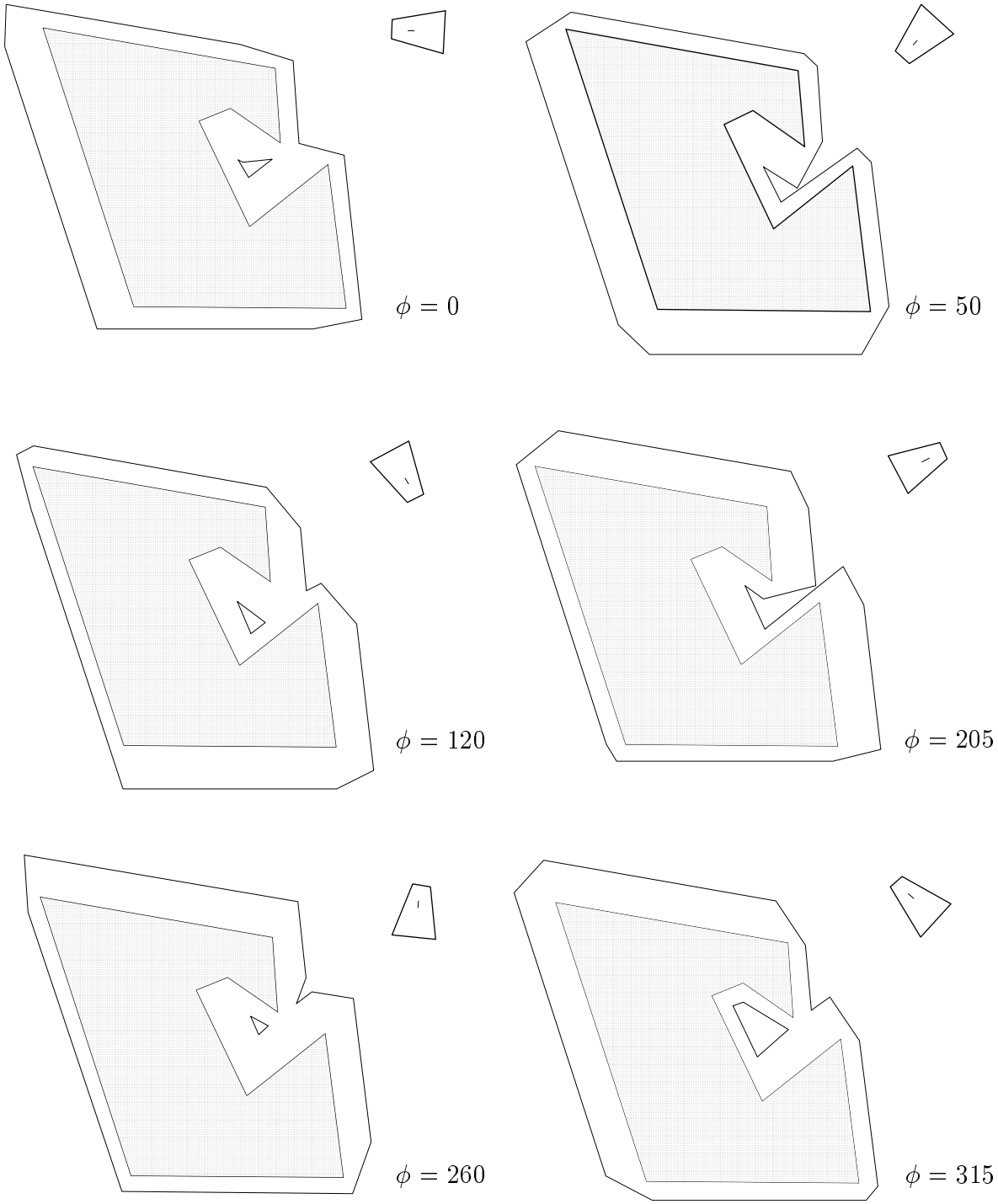

Figure 2.15: *Sections of the $\mathcal{C}$-space for different values of the orientation ϕ of the manipulated object.*

- Exact cell decomposition methods.
- Approximate cell decomposition methods.

The exact cell decomposition methods decompose $\mathcal{C}_{free}$ in cells whose union is $\mathcal{C}_{free}$. The approximate cell decomposition methods decompose $\mathcal{C}_{free}$ in cells of simple predefined shape whose union is strictly included into $\mathcal{C}_{free}$.

Although the approximate cell decomposition methods are simpler and easier to implement, they are not suitable when a characterization of the discontinuities of the motion constraints is required. This is the case for assembly tasks, since during their execution contacts may arise due to uncertainties and small celarances. Therefore, since this work deals with the automation of assembly tasks with robots, we use an exact cell decomposition method.

There are several exact decomposition methods which are reviewed in [62]. The following characteristics are desirable for any exact decomposition method:

- The cells must be simple enough in order to easily compute a path between any two configurations of a cell.
- The adjacency between cells must be easily tested and the path between two adjacent cells be easily found.

The method we are following is based in the work of Avanim et al. [4]. This method decomposes $\mathcal{C}_{free}$ and $\mathcal{C}_{contact}$, allowing the planning of motions in $\mathcal{C}_{free}$ and motions in $\mathcal{C}_{contact}$ in the same way.

2.6.1 Partition of the free-space

This Section describes the cell decomposition method used to partition $\mathcal{C}_{free}$. The definition of the cells used and the procedure to obtain the partition are as follows.

Definition 17: A *$\mathcal{C}$-prism* is the set of connected configurations of $\mathcal{C}_{free}$ that satisfy:

$$c = \alpha e_1(\phi) + \beta e_2(\phi) + \gamma e_3(\phi) \tag{2.35}$$

with

$$\begin{aligned} \alpha, \beta, \gamma &\in [0, 1] \\ \alpha + \beta + \gamma &= 1 \\ \phi &\in [\phi_{bottom}, \phi_{top}] \end{aligned} \tag{2.36}$$

e_1, e_2 and e_3 being three $\mathcal{C}$-edges of the $\mathcal{C}$-space, and $[\phi_{bottom}, \phi_{top}]$ the range of orientations were the three $\mathcal{C}$-edges simultaneously exist.

The $\mathcal{C}$-prisms allow the partition of the free-space since they are disjoint regions whose union is the free-space. They are simple enough in order to easily compute a path

between any two of their configurations, and the adjacency between $\mathcal{C}$-prisms can be easily determined. Therefore the $\mathcal{C}$-prisms are suitable for the construction of a path in $\mathcal{C}_{free}$.

Definition 18: A $\mathcal{C}$-slice is the set configurations of $\mathcal{C}_{free}$ with orientations $\phi \in [\phi_b, \phi_t]$, where ϕ_b and ϕ_t are two consecutive orientations of $\mathcal{C}$-vertices.

The top and the bottom orientations of a $\mathcal{C}$-prism correspond to the top or the bottom of a $\mathcal{C}$-slice since the $\mathcal{C}$-vertices are the extremes of the $\mathcal{C}$-edges. The algorithm to partition $\mathcal{C}_{free}$ in a set of $\mathcal{C}$-prisms is the following:

$\mathcal{C}_{free}$-Partition()

For the middle orientation of each $\mathcal{C}$-slice do:

Generate a triangular mesh of the corresponding section of $\mathcal{C}_{free}$

Associate to each triangle the three $\mathcal{C}$-edges that contain its vertices.

Go through all the $\mathcal{C}$-slices increasing the value of the orientation For each $\mathcal{C}$-slice s_i (with orientation range $[\phi_b^i, \phi_t^i]$) do:

Find the triangles that do not have an equivalent triangle in the previous slice s_{i-1} (being two triangle equivalent if they have the same set of associated $\mathcal{C}$-edges)

For each of these triangles t_k create a $\mathcal{C}$-prism:

$\phi_{bottom} = \phi_b^i$

Associate to the $\mathcal{C}$-prism the $\mathcal{C}$-edges associated to the triangle

Find the top orientation:

Go through all the $\mathcal{C}$-slices s_j with $\phi_b^j \geq \phi_t^i$. If the triangle t_k does not have an equivalent triangle in s_j then $\phi_{top} = \phi_b^j$

END

Figures 2.16a and 2.16b show the triangular mesh of two consecutive $\mathcal{C}$-slices s_i and s_j for an orientation $\phi = \phi_t^i = \phi_b^j$. Since one of the triangles of s_j do not exist in s_i, this orientation is the bottom orientation of a $\mathcal{C}$-prism, i.e. $\phi_{bottom} = \phi_b^j$. Figures 2.16c and 2.16d show the triangular mesh of two consecutive $\mathcal{C}$-slices s_k and s_l for an orientation $\phi = \phi_t^k = \phi_b^l$, being the triangle shown in Figure 2.16c the same as the one of Figure 2.16b (i.e. they have the same associated $\mathcal{C}$-edges). The top orientation of the $\mathcal{C}$-prism occurs for this orientation, i.e. $\phi_{top} = \phi_b^l$, since the triangle of s_k do not exist in s_l. Figure 2.17 shows the obtained $\mathcal{C}$-prism together with its associated $\mathcal{C}$-edges represented in $\mathcal{C}'$-space.

In order to plan a path in $\mathcal{C}_{free}$, let introduce the following concepts:

Definition 19: A *$\mathcal{C}_f$-border* is the set of configurations that belong to two $\mathcal{C}$-prisms.

Definition 20: A *$\mathcal{C}_f$-node* is the middle configuration of a $\mathcal{C}_f$-border.

Definition 21: A *$\mathcal{C}_f$-arc* is the path inside a $\mathcal{C}$-prism that connects two of its $\mathcal{C}_f$-nodes.

Definition 22: A *$\mathcal{C}_f$-graph* is a graph whose nodes represent $\mathcal{C}_f$-nodes and whose arcs represent $\mathcal{C}_f$-arcs. Each arc of $\mathcal{C}_f$-graph have an associated initial cost equal to the length of the $\mathcal{C}_f$-arc. This cost can be modified following some policies of the motion planning algorithm introduced in Section 2.7.

Definition 23: A *$\mathcal{C}_f$-path* is a sequence of $\mathcal{C}_f$-nodes connected by $\mathcal{C}_f$-arcs that link an initial $\mathcal{C}_f$-node with a goal $\mathcal{C}_f$-node.

The $\mathcal{C}_f$-graph associated to the $\mathcal{C}$-space of an assembly task is build from the set of $\mathcal{C}$-prisms that compose it in the following way:

- **Determination of the $\mathcal{C}_f$-nodes**:

  (1) Find the adjacency between $\mathcal{C}$-prisms. There is lateral adjacency between two $\mathcal{C}$-prisms if for a given $\mathcal{C}$-slice the associated triangles are adjacent, which is obtained from the algorithm used to generate the triangular mesh [88]. There is top/bottom adjacency if the top triangle of a $\mathcal{C}$-prism and the bottom triangle of another take place at the same orientation, and their intersection is not empty.

  (2) Compute the $\mathcal{C}_f$-node depending on the type of adjacency:

  (2.1) *Top/bottom adjacency*:
  The $\mathcal{C}_f$-border between two $\mathcal{C}$-prisms with top/bottom adjacency is defined by the set of configurations satisfying:

$$c = \sum_i \alpha_i p_i \tag{2.37}$$

  with

$$\begin{aligned} \alpha_i &\in [0,1] \\ \sum_i \alpha_i &= 1 \end{aligned} \tag{2.38}$$

  p_i being the intersection points of the two triangles corresponding to the top and the bottom of the $\mathcal{C}$-prisms that coincide in orientation. Then the $\mathcal{C}_f$-node is the barycenter of the polygon with vertices p_i (Figure 2.18a).

  (2.2) *Lateral adjacency*:
  The $\mathcal{C}_f$-border between two $\mathcal{C}$-prisms with lateral adjacency is defined by the set of configurations satisfying:

$$c = \alpha e_1(\phi) + \beta e_2(\phi) \tag{2.39}$$

  with

$$\begin{aligned} \alpha, \beta &\in [0,1] \\ \alpha + \beta &= 1 \\ \phi &\in [\phi_{pm}, \phi_{pM}] \end{aligned} \tag{2.40}$$

  e_1 and e_2 being the two common $\mathcal{C}$-edges, and $[\phi_{pm}, \phi_{pM}]$ the range of orientations were the two $\mathcal{C}$-prisms simultaneously exist. Then, if $\phi_n = (\phi_{pm} + \phi_{pM})/2$, the $\mathcal{C}_f$-node is the middle point of the segment with extremes $e_2(\phi_n)$ and $e_1(\phi_n)$ (Figure 2.18b).

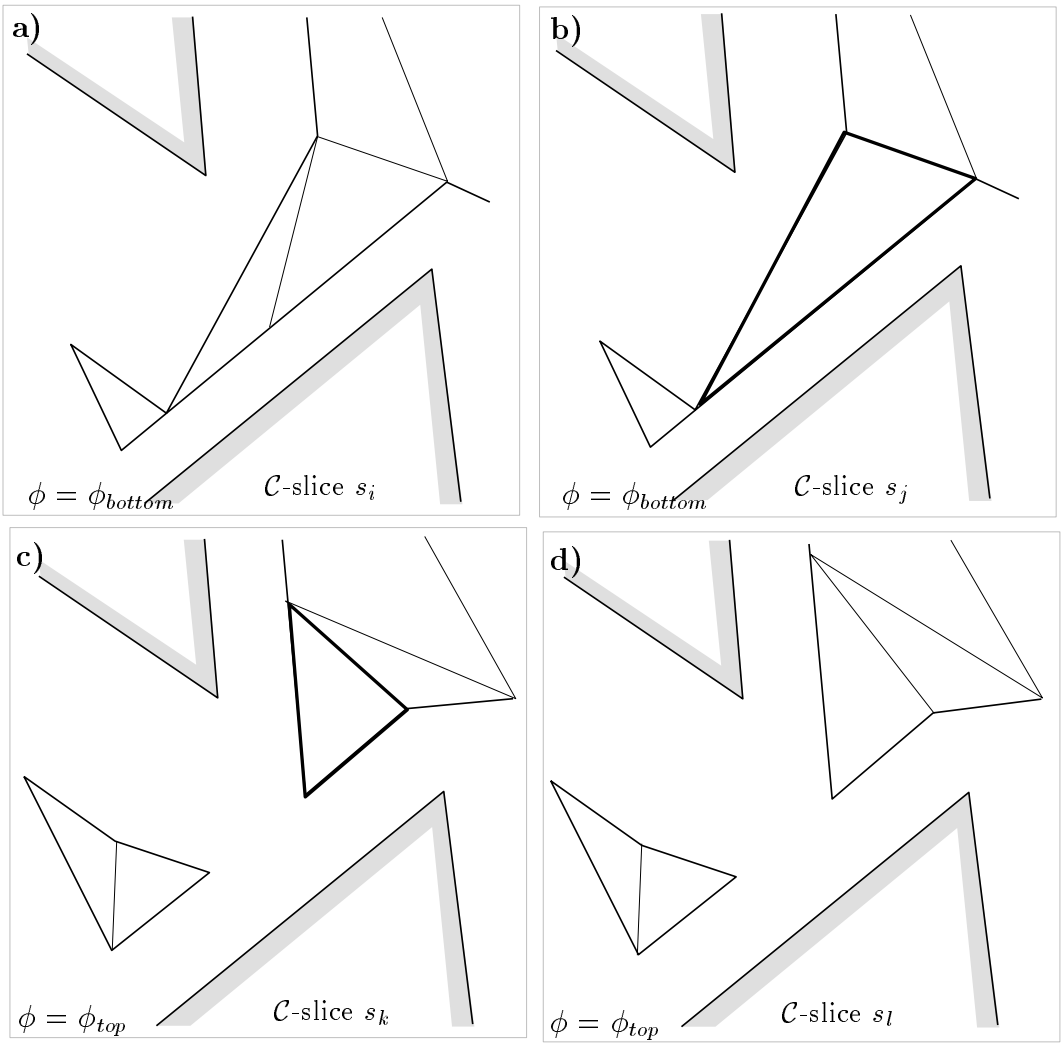

Figure 2.16: *Triangular mesh of two consecutive $\mathcal{C}$-slices defining the bottom orientation of a $\mathcal{C}$-prism (Figures a and b). Triangular mesh of two consecutive $\mathcal{C}$-slices defining the top orientation of the same $\mathcal{C}$-prism (Figures c and d). The bottom and top triangles of the $\mathcal{C}$-prism are shown in Figures b and c, respectively.*

- **Determination of the $\mathcal{C}_f$-arcs**:
  The $\mathcal{C}_f$-arc between two $\mathcal{C}_f$-nodes $n_i = (x_i, y_i, \phi_i)$ and $n_g = (x_g, y_g, \phi_g)$ is computed as follows. Let $e_1(\phi) = (x_1(\phi), y_1(\phi), \phi)$, $e_2(\phi) = (x_2(\phi), y_2(\phi), \phi)$ and $e_3(\phi) = (x_3(\phi), y_3(\phi), \phi)$ be the three configurations of the $\mathcal{C}$-edges associated to the $\mathcal{C}$-prism for orientation ϕ. The configurations n_i and n_g satisfy:

$$\begin{aligned} \overrightarrow{e_1 n_i} &= \alpha_i \overrightarrow{e_2 e_1} + \beta_i \overrightarrow{e_3 e_1} \\ \overrightarrow{e_1 n_g} &= \alpha_g \overrightarrow{e_2 e_1} + \beta_g \overrightarrow{e_3 e_1} \end{aligned} \tag{2.41}$$

  Then, any configuration c of the arc satisfies:

$$\overrightarrow{e_1 c} = \alpha(\phi) \overrightarrow{e_2 e_1} + \beta(\phi) \overrightarrow{e_3 e_1} \tag{2.42}$$

  with

$$\alpha(\phi) = \alpha_i + (\alpha_g - \alpha_i) \frac{\phi - \phi_i}{\phi_g - \phi_i}$$

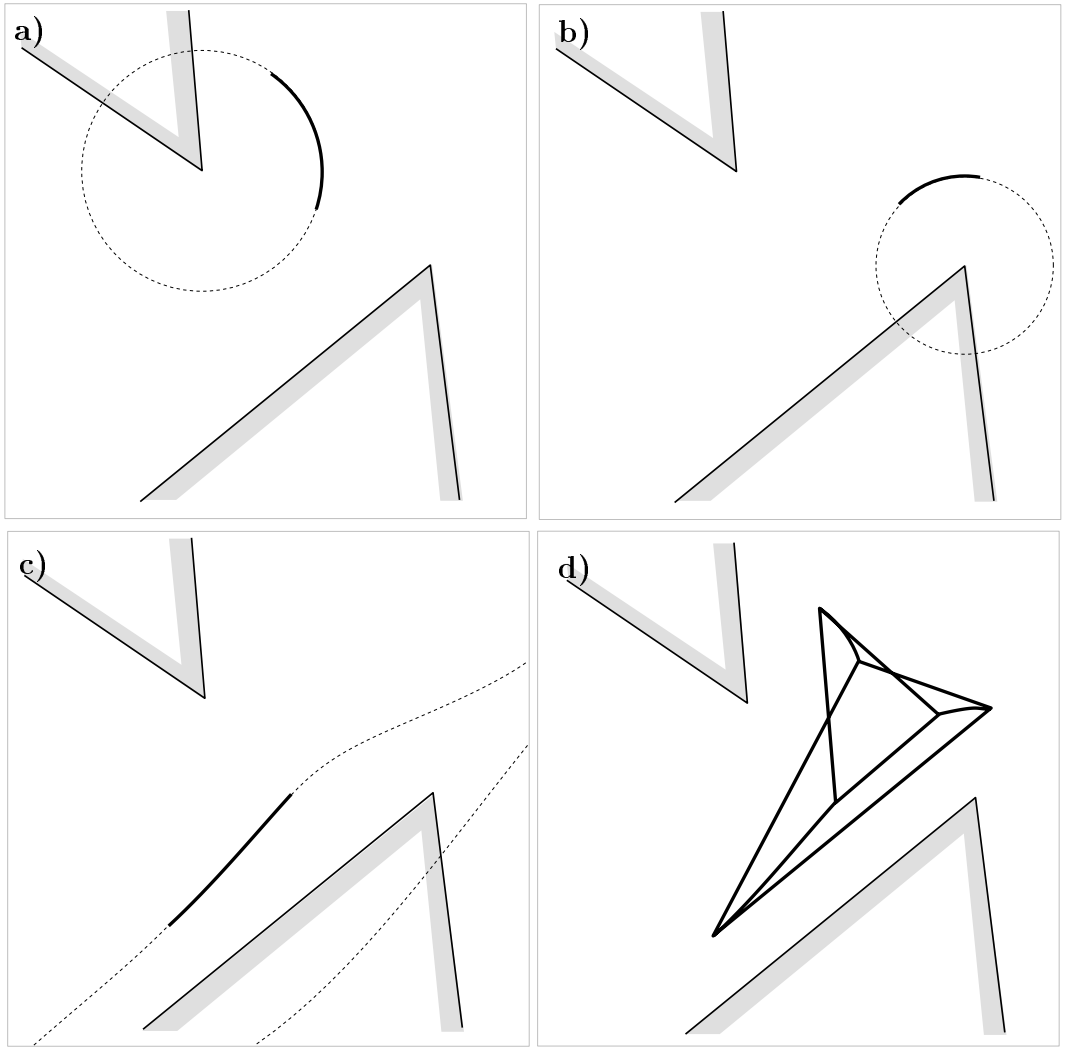

Figure 2.17: *Representation in $\mathcal{C}'$-space of a $\mathcal{C}$-prism (d) and its associate $\mathcal{C}$-edges (a, b and c).*

$$\beta(\phi) = \beta_i + (\beta_g - \beta_i)\frac{\phi - \phi_i}{\phi_g - \phi_i} \tag{2.43}$$

where α_i, α_g, β_i and β_g are determined by equation (2.41). The arc can also be expressed as:

$$\begin{aligned} x(\phi) &= x_1(\phi) + \alpha(\phi)[x_2(\phi) - x_1(\phi)] + \beta(\phi)[x_3(\phi) - x_1(\phi)] \\ y(\phi) &= y_1(\phi) + \alpha(\phi)[y_2(\phi) - y_1(\phi)] + \beta(\phi)[y_3(\phi) - y_1(\phi)] \\ q(\phi) &= \rho\phi \end{aligned} \tag{2.44}$$

2.6.2 Partition of the contact-space

Contact motions reduce the degrees of freedom and thus reduce the uncertainties, being desirable in assembly tasks. If two objects are in contact at a given configuration, it is possible to move them to another contact configuration through contact motions [54].

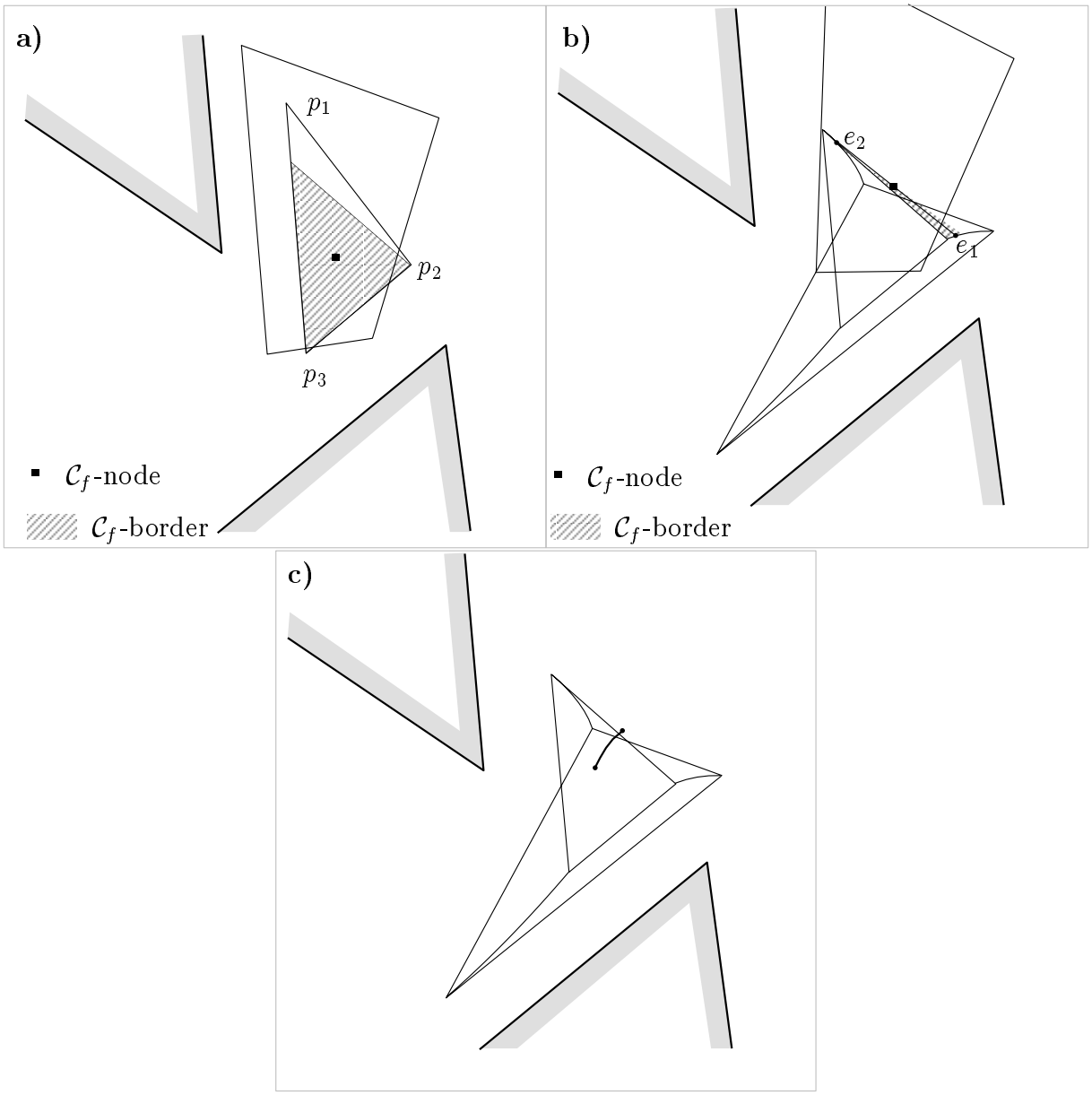

Figure 2.18: *a) $\mathcal{C}_f$-node of a $\mathcal{C}$-prism corresponding to a top/bottom adjacency b) $\mathcal{C}_f$-node of a $\mathcal{C}$-prism corresponding to a lateral adjacency) $\mathcal{C}_f$-arc connecting the previous $\mathcal{C}_f$-nodes.*

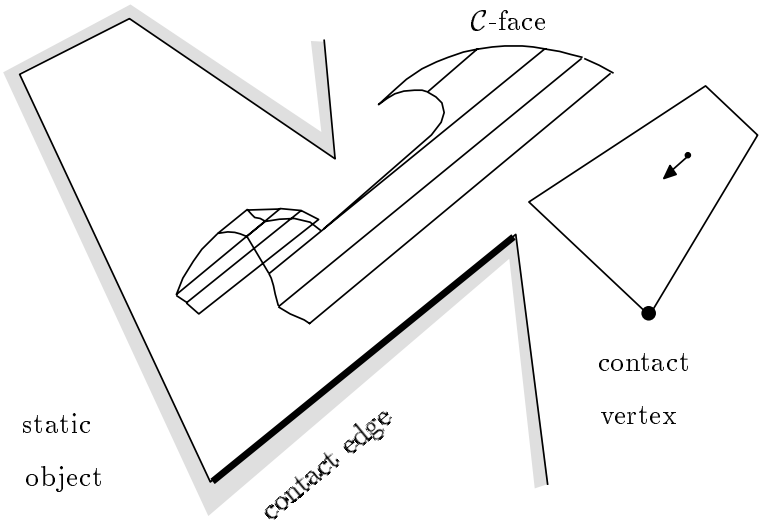

Figure 2.19: *$\mathcal{C}$-items of a $\mathcal{C}$-face.*

In the $\mathcal{C}$-space construction algorithm presented in section 2.5.1, the $\mathcal{C}$-faces were divided into a set of $\mathcal{C}$-items, being the $\mathcal{C}$-items non-overlapping regions whose union is the $\mathcal{C}$-face (Figure 2.19). Therefore, the $\mathcal{C}$-space construction algorithm presented in section 2.5.1 is an exact cell decomposition method for $\mathcal{C}_{contact}$.

The $\mathcal{C}$-items introduced in Definition 15, are defined again for convenience.

Definition 24: A *$\mathcal{C}$-item* is the set of connected configurations of $\mathcal{C}_{contact}$ that satisfy:

$$c = \alpha e_1(\phi) + \beta e_2(\phi) \tag{2.45}$$

with

$$\begin{aligned} \alpha, \beta &\in [0, 1] \\ \alpha + \beta &= 1 \\ \phi &\in [\phi_{bottom}, \phi_{top}] \end{aligned} \tag{2.46}$$

e_1 and e_2 being two $\mathcal{C}$-edges of the $\mathcal{C}$-space, and $[\phi_{bottom}, \phi_{top}]$ the range of orientations were the two $\mathcal{C}$-edges simultaneously exist.

Then, the $\mathcal{C}$-items are simple enough in order to easily compute a path between any two of their configurations, and the adjacency between $\mathcal{C}$-items is easily determined (section 2.5.1). Therefore the $\mathcal{C}$-items are suitable for the construction of a path in $\mathcal{C}_{contact}$.

Let introduce the following concepts for motion planning in $\mathcal{C}_{contact}$ in a similar way as the ones defined for $\mathcal{C}_{free}$:

Definition 25: A *$\mathcal{C}_c$-border* is the set of configurations that belong to two $\mathcal{C}$-items.

Definition 26: A *$\mathcal{C}_c$-node* is the middle configuration of a $\mathcal{C}_c$-border (Figure 2.20a).

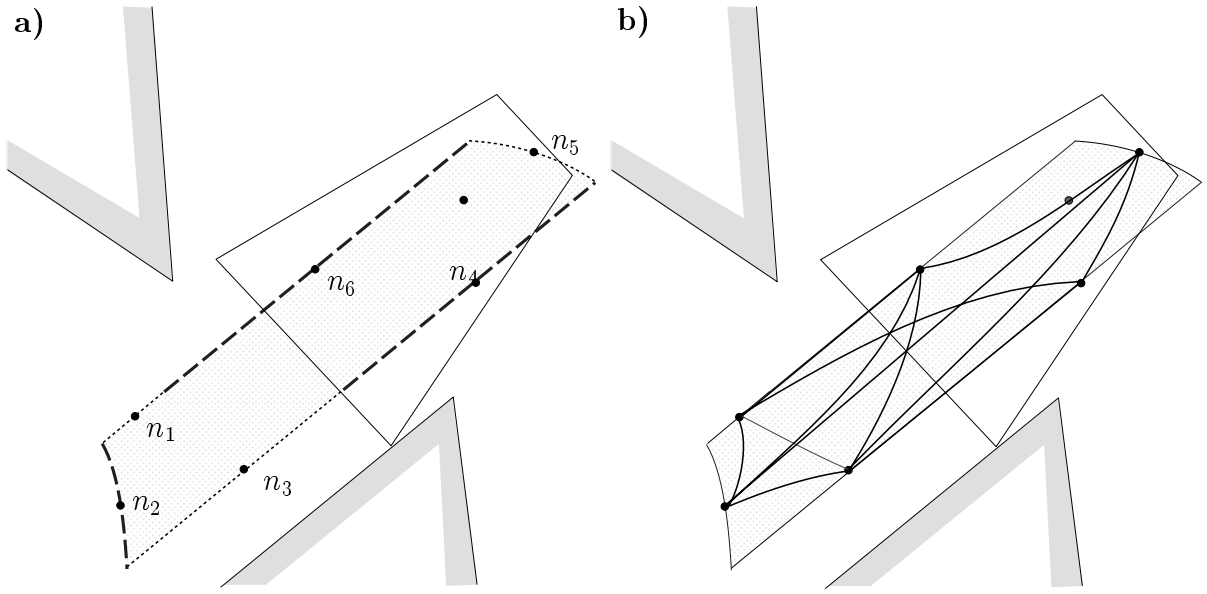

Figure 2.20: *a) $\mathcal{C}_c$-nodes of a $\mathcal{C}$-item b) $\mathcal{C}_c$-arcs of a $\mathcal{C}$-item.*

Definition 27: A *$\mathcal{C}_c$-arc* is the path over a $\mathcal{C}$-item that connects two of its $\mathcal{C}_c$-nodes (Figure 2.20b).

Definition 28: A *$\mathcal{C}_c$-graph* is a graph whose node represent $\mathcal{C}_c$-nodes and whose arcs represent $\mathcal{C}_c$-arcs. Each arc of $\mathcal{C}_c$-graph have an associated initial cost equal to the length of the $\mathcal{C}_c$-arc. This cost can be modified following some policies of the motion planning algorithm introduced in Section 2.7.

Definition 29: A *$\mathcal{C}_c$-path* is a sequence of $\mathcal{C}_c$-nodes connected by $\mathcal{C}_c$-arcs that link an initial $\mathcal{C}_c$-node with a goal $\mathcal{C}_c$-node.

The $\mathcal{C}_c$-graph associated to the $\mathcal{C}$-space of an assembly task is build from the set of $\mathcal{C}$-items that compose it in the following way:

- **Determination of the $\mathcal{C}_c$-nodes**:
  First the $\mathcal{C}_c$-borders between the adjacent $\mathcal{C}$-items are determined. The $\mathcal{C}_c$-borders are arcs of curves in $\mathcal{C}$-space with extremes at some given orientations ϕ_m and ϕ_M.
  - If $\phi_m \neq \phi_M$: the $\mathcal{C}_c$-border is a $\mathcal{C}$-edge and the $\mathcal{C}_c$-node is the point of the $\mathcal{C}$-edge for the orientation $(\phi_m + \phi_M)/2$ (e.g. the nodes n_2 and n_5 in Figure 2.20a).
  - If $\phi_m = \phi_M$: the $\mathcal{C}_c$-border is a segment of a straigth line (which may be a $\mathcal{C}$-edge or not), and the $\mathcal{C}_c$-node associated to it is the middle point of the segment (e.g. the nodes n_1, n_6, n_2 and n_4 in Figure 2.20a).
- **Determination of the $\mathcal{C}_c$-arcs**:
  The $\mathcal{C}_c$-arc between two $\mathcal{C}_c$-nodes $n_i = (x_i, y_i, \phi_i)$ and $n_g = (x_g, y_g, \phi_g)$ is computed as follows. Let $e_1(\phi) = (x_1(\phi), y_1(\phi), \phi)$ and $e_2(\phi) = (x_2(\phi), y_2(\phi), \phi)$ be the two configurations of the $\mathcal{C}$-edges associated to the $\mathcal{C}$-item for orientation ϕ. The

configurations n_i and n_g satisfy:

$$\overrightarrow{e_1 n_i} = \alpha_i \overrightarrow{e_2 e_1} \quad (2.47)$$
$$\overrightarrow{e_1 n_g} = \alpha_g \overrightarrow{e_2 e_1} \quad (2.48)$$

Then, any configuration c of the $\mathcal{C}_c$-arc satisfies:

$$\overrightarrow{e_1 c} = \alpha(\phi) \overrightarrow{e_2 e_1} \quad (2.49)$$

with

$$\alpha(\phi) = \alpha_i + (\alpha_g - \alpha_i)\frac{\phi - \phi_i}{\phi_g - \phi_i} \quad (2.50)$$

where α_i and α_g are determined by equation (2.47) and (2.48), respectively. The $\mathcal{C}_c$-arc can also be expressed as:

$$\begin{aligned} x(\phi) &= x_1(\phi) + \alpha(\phi)(x_2(\phi) - x_1(\phi)) \\ y(\phi) &= y_1(\phi) + \alpha(\phi)(y_2(\phi) - y_1(\phi)) \\ q(\phi) &= \rho\phi \end{aligned} \quad (2.51)$$

The $\mathcal{C}_c$-arcs are completely inside the $\mathcal{C}$-item and have an associated value which is the distance between the connected $\mathcal{C}_c$-nodes, computed as the length of the arc of curve represented by the $\mathcal{C}_c$-arc.

2.7 Motion planning algorithm

Given a goal node and an initial node of a graph, either $\mathcal{C}_f$-graph or $\mathcal{C}_c$-graph, the Dijkstra algorithm (Appendix A) is applied in order to compute the path of minimum cost. The Dijkstra algorithm is applied to any two pairs of nodes of the $\mathcal{C}_c$-graph and to any two pairs of the nodes of the $\mathcal{C}_f$-graph. As a result, all the possible $\mathcal{C}_c$-paths and all the possible $\mathcal{C}_f$-paths are obtained.

2.7.1 Search policies

Some policies can be defined in order to determine the type of $\mathcal{C}$-paths obtained, by increasing or decreasing the value of the cost associated to some given $\mathcal{C}$-arcs. Some possible policies are enumerated:

1. Avoid the $\mathcal{C}$-arcs that are over a $\mathcal{C}$-edge corresponding to a vertex-vertex contact by setting to infinity the cost of the arc in the $\mathcal{C}$-graph.

2. Penalize the $\mathcal{C}$-arcs with a $\mathcal{C}$-node that is over a $\mathcal{C}$-edge corresponding to a vertex-vertex contact by setting to a great value the cost of the arc in the $\mathcal{C}$-graph.

3. Favour/Penalize the $\mathcal{C}$-arcs corresponding to pure translations/rotations, by multiplying by a factor less/greater than 1 the cost of the arc in the $\mathcal{C}$-graph.

4. Favour/Penalize the $\mathcal{C}$-arcs corresponding to motions that maintain one/two basic contacts, by multiplying by a factor less/greater than 1 the cost of the arc in the $\mathcal{C}$-graph.

5. Avoid a given $\mathcal{C}$-arc by setting to infinity the cost of the arc in the $\mathcal{C}$-graph.

2.7.2 Performance

The fine motion planning algorithm has been implemented in C++ on a Silicon Graphics workstation (175 MHz R10000 Indigo 2). The assembly task used as example is that of the figures shown, being composed of 341 $\mathcal{C}_c$-nodes and 746 $\mathcal{C}_f$-nodes. The CPU time to compute the $\mathcal{C}_c$-paths from any $\mathcal{C}_c$-node to any $\mathcal{C}_c$-node of $\mathcal{C}_c$-graph is 3.68 seconds, and the CPU time to compute the $\mathcal{C}_f$-paths from any $\mathcal{C}_f$-node to any $\mathcal{C}_f$-node of $\mathcal{C}_f$-graph is 34.43 seconds.

2.8 Analysis of reaction forces

In this Section reaction forces will be analyzed, since they may arise during the motions in $\mathcal{C}_{contact}$. A reaction force $\vec{f} = [f_x \quad f_y]^T$ resulting from a contact situation during a planar assembly task and producing a torque τ with respect to the manipulated object reference point, can be represented in a tridimensional force space $\mathcal{F}_3$ by a generalized reaction force $\vec{g} = [f_x \quad f_y \quad f_q]^T$, with $f_q = \frac{\tau}{\rho}$, being ρ the radius of gyration (Section 2.1).

2.8.1 Force decomposition

In the absence of friction, the reaction force arising at a contact situation involving one basic contact is in the direction normal to the $\mathcal{C}$-face at the contact point. This Section analyzes the effect of friction and of an applied generalized force, in order to find the reaction force that arises at the basic contact.

Definition 30: The *tangent plane* Π_t associated to a given contact configuration c_o of a basic contact i, is the plane tangent to $\mathcal{F}_i$ at c_o.

Π_t is defined by the direction $\vec{n}$ normal to the $\mathcal{C}$-face at the contact configuration. If $(n_x, n_y) = (\cos\psi_W, \sin\psi_W)$ is the normal to the contact edge, and (r_x, r_y) is the vector from the contact point to the manipulated object reference point, then $\vec{n}$ has the following expression:

$$\vec{n} = (n_x, n_y, n_q/\rho) \tag{2.52}$$

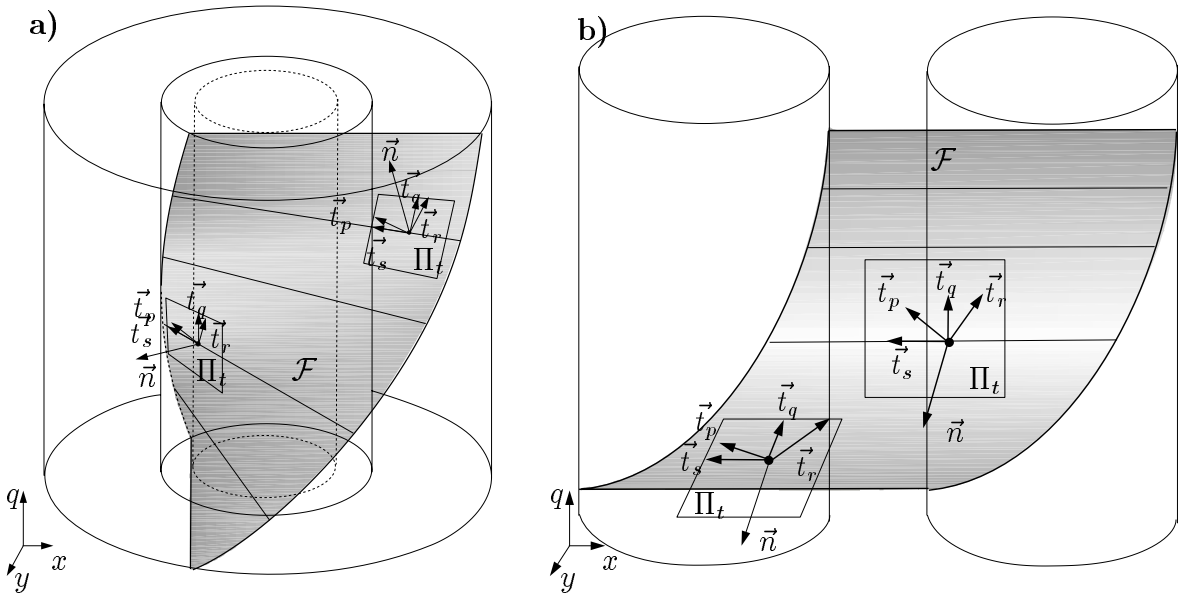

Figure 2.21: *Contact reference frames in a type-A and in a type-B basic contacts.*

where:

$$n_q = n_x r_y - n_y r_x \tag{2.53}$$

At any contact configuration, the directions of motion that instantaneously maintain the contact are those that belong to the tangent plane. The following directions belonging to the tangent plane Π_t will be of interest (Figure 2.21):

a) *Direction* $\vec{t}_r$: Direction of pure rotation about the contact point:

$$\vec{t}_r = (-r_y, r_x, \rho) \tag{2.54}$$

A positive motion along $\vec{t}_r$ corresponds to a rotation that increases the orientation ϕ of the manipulated object.

b) *Direction* $\vec{t}_p$: Direction perpendicular to $\vec{t}_r$ and $\vec{n}$, The sense of $\vec{t}_p$ is such that $[\vec{t}_r, \vec{t}_p, \vec{n}]$ is a right-handed frame.

c) *Direction* $\vec{t}_s$: Direction of pure sliding:

$$\vec{t}_s = \pm(n_y, -n_x, 0) \tag{2.55}$$

d) *Direction* $\vec{t}_q$: Direction perpendicular to $\vec{t}_s$. A positive motion along $\vec{t}_q$ corresponds to a rotation that increases the orientation ϕ of the manipulated object.

The sense of $\vec{t}_s$ is such that the frame $[\vec{t}_q, \vec{t}_s, \vec{n}]$ is a right-handed frame

Definition 31: The *contact reference frame* is the orthogonal reference frame $[\vec{t}_r, \vec{t}_p, \vec{n}]$ with its origin at the contact configuration.

The contact reference frame allows the vectorial decomposition of an applied force in order to analyze its effect on the movement of the manipulated object [38]. Figures 2.21a and 2.21b show the contact reference frame for type-A and type-B basic contacts, respectively, corresponding to different contact configurations. In each contact configuration, the tangent plane Π_t is drawn together with the directions $\vec{t}_r$, $\vec{t}_p$, $\vec{t}_s$ and $\vec{t}_q$.

The effect of friction for planar assembly tasks in the tridimensional $\mathcal{C}$-space has been studied in depth by Erdamnn [38], who introduces the generalized friction cone.

Definition 32: The *generalized friction cone* is the range of possible generalized reaction force directions arising from a basic contact in a given contact configuration.

The generalized friction cone is a bidimensional cone in $\mathcal{C}$-space, determined by $\vec{n} \pm \mu\vec{v}_f$, $\vec{n}$ being the direction normal to the $\mathcal{C}$-face defined in equation (2.52), $\vec{v}_f$ the generalized friction vector, and μ the friction coefficient:

$$\vec{v}_f = (n_y, -n_x, v_q/\rho) \tag{2.56}$$

with $v_q = n_x r_x + n_y r_y$. The unitary vectors in the directions of the generalized friction cone edges defined by $(\vec{n} + \mu\vec{v}_f)$ and $(\vec{n} - \mu\vec{v}_f)$, will be noted by $\vec{e}^{\,+}$ and $\vec{e}^{\,-}$, respectively:

$$\begin{aligned} \vec{e}^{\,-} &= (n_x - \mu n_y,\ n_y + \mu n_x,\ [r_y(n_x - \mu n_y) - r_x(n_y + \mu n_x)]/\rho) \\ \vec{e}^{\,+} &= (n_x + \mu n_y,\ n_y - \mu n_x,\ [r_y(n_x + \mu n_y) - r_x(n_y - \mu n_x)]/\rho) \end{aligned} \tag{2.57}$$

Definition 33: The *friction plane* Π_f is the plane that contains the generalized friction cone. The direction normal to Π_f is the direction of pure rotation $\vec{t}_r$.

Definition 34: The *rotation plane* Π_r is the plane that contains the directions $\vec{t}_r$ and $\vec{n}$. The direction normal to Π_r is the direction $\vec{t}_p$.

The effect of an applied force when the manipulated object is in a one-point contact with the environment can be analyzed by decomposing that force, making use of the contact reference frame. As a result, a net force in the direction of motion and a reaction force are obtained.

Let $\vec{g}_A$ be the applied generalized force that points into the $\mathcal{C}$-face associated to the basic contact. $\vec{g}_A$ can be decomposed in the following way

$$\vec{g}_A = \vec{g}_f + \vec{g}_{t_r} \tag{2.58}$$

$\vec{g}_f$ being the component on the plane Π_f and $\vec{g}_{t_r}$ the component along the direction $\vec{t}_r$, perpendicular to Π_f.

Proposition 6: *The reaction force $\vec{g}_R$ produced in a basic contact is $\vec{g}_R = -\vec{g}_f$ if $\vec{g}_f$ is inside the generalized friction cone, or the negated projection of $\vec{g}_f$ along $\vec{t}_p$ onto the edge of the friction cone, otherwise.*

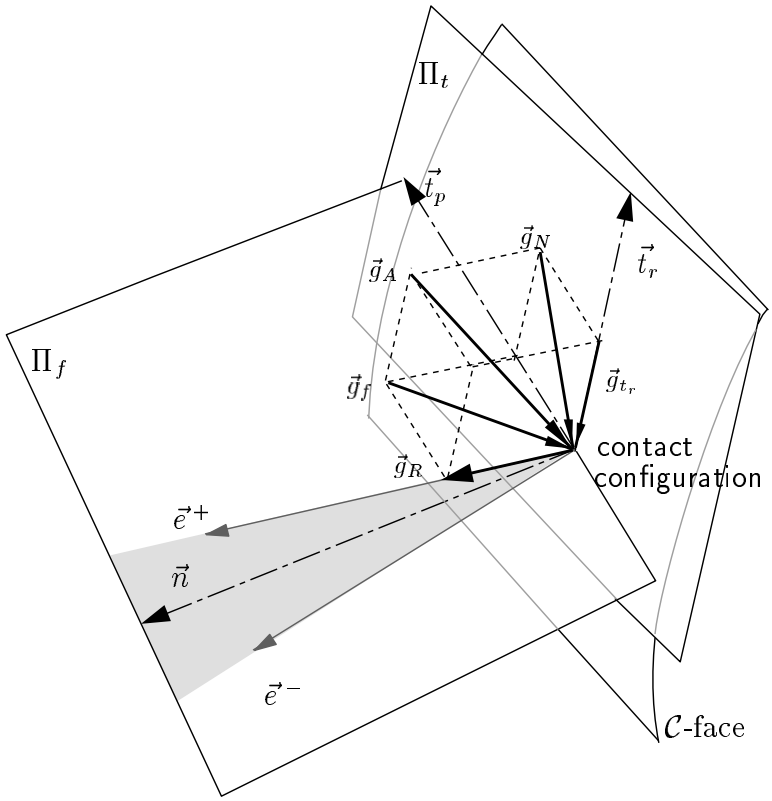

Figure 2.22: *Force decomposition.*

Proof: The generalized friction cone, which represent the possible reaction forces arising from a contact, lies in the plane Π_f. Then $\vec{g}_f$, the projection of $\vec{g}_A$ into Π_f, is the component of $\vec{g}_A$ that can be cancelled by a reaction force. If $\vec{g}_f$ lies inside the generalized friction cone, a reaction force arises cancelling it, i.e. $\vec{g}_R = -\vec{g}_f$. Otherwise only the projection of $\vec{g}_f$ onto the edge of the friction cone can be cancelled by a reaction force in the direction of this edge. ◇

Proposition 7: *The net force $\vec{g}_N$ that defines the direction of motion is the projection of $\vec{g}_A$ along the direction determined by $\vec{g}_R$ into the plane Π_t.*

Proof: The net force $\vec{g}_N$ defines the direction of motion over the plane Π_t since it is the component of the applied force which is not cancelled by the reaction force, then $\vec{g}_N = \vec{g}_A + \vec{g}_R$, i.e. it is the projection of $\vec{g}_A$ into the plane Π_t along the direction determined by $\vec{g}_R$. ◇

Figure 2.22 shows the force decomposition of an applied force $\vec{g}_A$.

For contact situations involving more than one basic contact, the range of possible generalized reaction force directions, i.e. the composite friction cone, is the vector sum of the range of possible generalized reaction force directions arising at each basic contact in the given contact configuration, i.e. the vector sum of each friction cone.

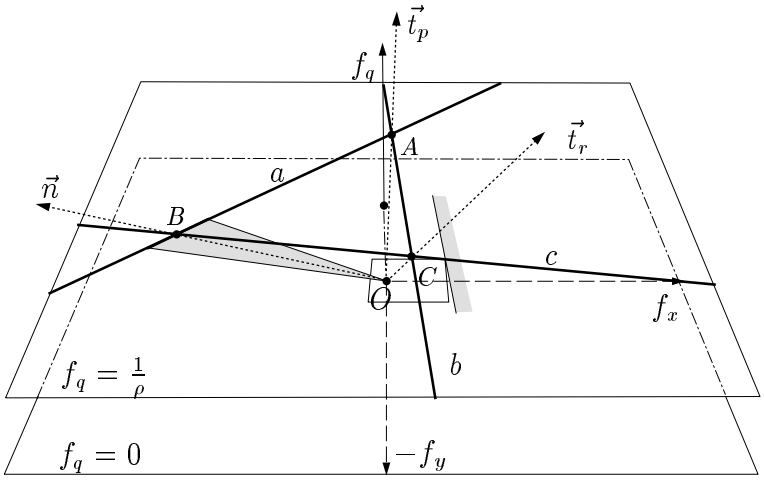

Figure 2.23: *Intersection of the contact reference frame with the plane* $f_q = \frac{1}{\rho}$.

2.8.2 Force decomposition in the dual plane

Generalized forces will be represented using the dual representation of forces [14] (Appendix B). The dual representation of forces is a graphical method that can be used for the analysis of planar contact problems, since it transforms planar motions and forces to the corresponding *acceleration centers*. This representation maps a line of force into a point of a plane that expresses the line direction, and a sign that expresses its sense.

Definition 35: The *dual plane* is the plane composed of dual points of forces.

Let define:

π'_t : the line composed of the dual points of the forces that belong to the tangent plane Π_t.

π'_f : the line composed of the dual points of the forces that belong to the friction plane Π_f.

π'_r : the line composed of the dual points of the forces that belong to the rotation plane Π_r.

T'_p : the dual representation of the direction $\vec{t}_p$.

N' : the dual representation of the direction $\vec{n}$.

T'_r : the dual representation of the direction $\vec{t}_r$.

Figure 2.23 shows the generalized force space where the plane $f_q = \frac{1}{\rho}$ has been drawn in order to illustrate its intersection with the contact reference frame and the planes defined by it. The points A, B and C correspond to the intersection of the plane $f_q = \frac{1}{\rho}$ with the axis of the contact reference frame defined by the vectors $\vec{t}_p$, $\vec{n}$ and $\vec{t}_r$, respectively. The lines a, b, and c correspond to the intersection of the plane $f_q = \frac{1}{\rho}$ with the planes Π_f, Π_t and Π_r, respectively.

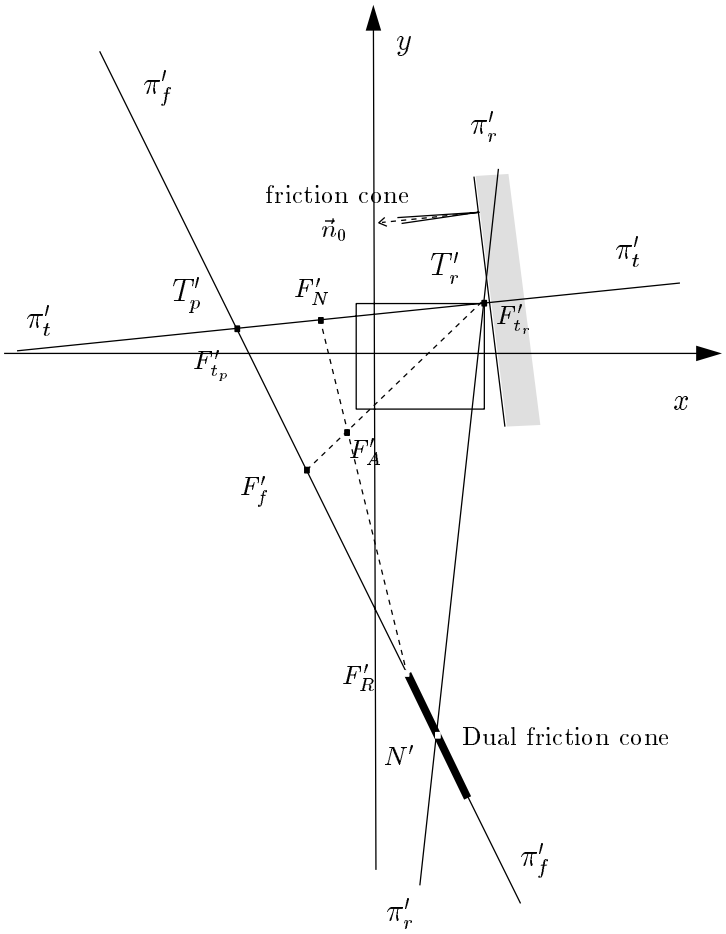

Figure 2.24: *Force decomposition in the dual plane.*

A $\pi/2$ counterclockwise rotation of the plane $f_q = \frac{1}{\rho}$ in Figure 2.23 around axis f_q coincides with the dual representation of the contact situation. Figure 2.24 shows this dual representation where it can be seen that the points A, B and C give rise to the dual points T'_p, N' and T'_r, respectively, and the lines a, b and c give rise to the lines π'_f, π'_t and π'_r, respectively. The generalized friction cone is represented by a segment of π'_r called the dual friction cone.

Some properties of the dual representation are illustrated in Appendix B. Other properties that will be used for the decomposition of an applied force are the following:

Property 8: The dual representation T'_r of the direction of pure rotation $\vec{t_r}$ coincides with the contact point, since it represents the acceleration center.

Property 9: A plane Π and its normal direction $\vec{n}$ in $\mathcal{F}_3$ are mapped in the dual plane into a line π' and a point N' that maintain between them a relation of duality, i.e. N' can be obtained by computing the dual expression of π'.

Property 10: Let $\vec{g}_p$ be the projection of a vector $\vec{g}$ into a plane Π_p along a given direction $\vec{t}$, and $\vec{g}_t$ the component along $\vec{t}$, i.e. $\vec{g} = \vec{g}_p + \vec{g}_t$; and let F', F'_p, F'_t, T' and

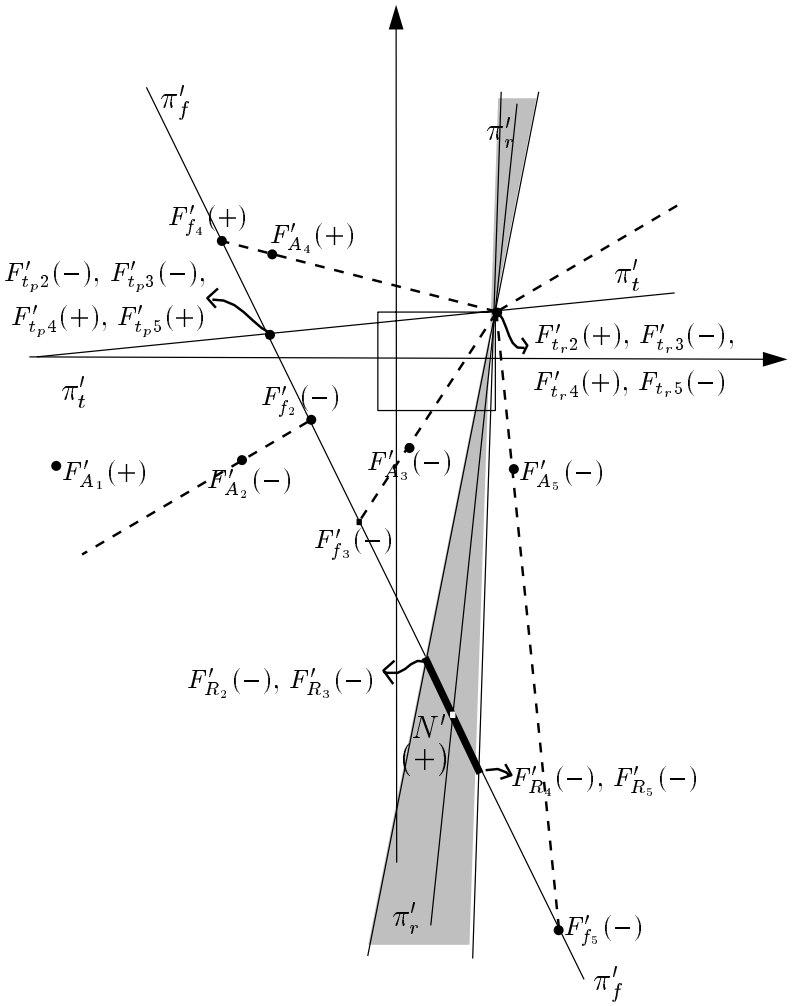

Figure 2.25: *a)* F'_{A_1} *looses contact while the other applied forces maintain it. b)* $F_{A'_2}$ *and* F'_{A_4} *produce a positive rotation about the contact point while* F'_{A_3} *and* F'_{A_5} *produce a negative one. c)* F'_{A_4} *and* F'_{A_5} *produce positive sliding while* F'_{A_2} *and* F'_{A_3} *produce negative sliding.*

π'_p be the dual representations of $\vec{g}$, $\vec{g}_p$, $\vec{g}_t$, $\vec{t}$ and Π_p, respectively. Then, F'_p is the intersection of π'_p and the line that contains F' and T', and F' satisfies $F' \in \overline{F'_p F'_t}$[2].

From Proposition 7 and Property 10, the dual representation F'_N of $\vec{g}_N$ is computed in the dual plane as the intersection of π'_t and the line that contains F'_A and F'_R. Figure 2.24 shows the dual representation of the force decomposition of Figure 2.22, where the dual lines π'_t, π'_f and π'_r represent the planes defined by the *contact reference frame* (Π_t, Π_f and Π_r, respectively).

[2]If $sign(F'_p) \neq sign(F'_t)$ then the segment is not finite [14].

2.8.3 Partition of the dual plane

The dual lines π'_t, π'_f and π'_r representing the planes defined by the *contact reference frame* (Π_t, Π_f and Π_r, respectively), partition the dual plane into regions. These regions bound the directions of applied forces that produce similar movements of the manipulated object (i.e. produce the same sense of sliding and rotation about the contact point, or produce sticking at it). Let a manipulated object be located at a one-basic contact configuration and be subject to an applied force $\vec{g}_A$.

Contact maintenance condition:

The manipulated object either moves along a direction contained in the tangent plane or sticks at the contact configuration if $\vec{g}_A$ satisfies $\vec{g}_A \cdot \vec{n} < 0$.

Let π_t^+ and π_t^- be the half-planes defined by π'_t such that $\pi_t^+ \supset N'$ if $sign(N') > 0$ and $\pi_t^- \supset N'$ if $sign(N') < 0$. Then, the contact maintenance condition is verified in the dual plane by testing $F'_A \in \pi_t^+$ if $sign(F'_A) < 0$ or $F'_A \in \pi_t^-$ if $sign(F'_A) > 0$.

Rotation Condition:

If $\vec{g}_A$ satisfies the contact maintenance condition, the manipulated object rotates clockwise around the contact vertex if $\vec{g}_A \cdot \vec{t_r} > 0$, and counter-clockwise otherwise.

Let π_f^+ and π_f^- be the half-planes defined by π'_f such that $\pi_f^+ \supset T'^3_r$. Then, the rotation condition is verified in the dual plane as follows:

- The manipulated object rotates clockwise around the contact vertex if $F'_A \in \pi_f^+$ when $sign(F'_A) > 0$ or $F'_A \in \pi_f^-$ when $sign(F'_A) < 0$.
- The manipulated object rotates counter-clockwise around the contact vertex if $F'_A \in \pi_f^-$ when $sign(F'_A) > 0$ or $F'_A \in \pi_f^+$ when $sign(F'_A) < 0$.

Sliding Condition:

If $\vec{g}_A$ satisfies the contact maintenance condition, the manipulated object sticks at the contact vertex if the projection of $\vec{g}_A$ into the friction plane lies inside the friction cone. Otherwise, the motion has a component:

- in the direction $\vec{t_p}$ and produces a reaction force in the direction e^- if $\vec{g}_A \cdot \vec{t_p} > 0$,
- in the direction opposite $\vec{t_p}$ and produces a reaction force in the direction e^+ if $\vec{g}_A \cdot \vec{t_p} < 0$.

Let π_r^0 be the region of dual points whose projection onto the line π'_r lie inside the dual friction cone. Region π_r^0, called the sticking region, is the cone built with the two lines that contain T'_r and one of the extremes of the dual friction cone. Let π_r^+ and π_r^- be the half-planes defined by π'_r such that $\pi_r^+ \supset T'_p$ if $sign(T'_p) > 0$ and $\pi_r^- \supset T'_p$ if $sign(T'_p) < 0$.

Then, the sliding condition is verified in the dual plane by first testing if $F'_A \in \pi_r^0$. If this

[3] By construction $sign(T'_r)$ is always positive.

is not satisfied:

- The motion has a component in the direction $\vec{t_p}$ if $F'_A \in \pi_r^+$ when $sign(F'_A) > 0$ or if $F'_A \in \pi_r^-$ when $sign(F'_A) < 0$.
- The motion has a component in the direction opposite $\vec{t_p}$ if $F'_A \in \pi_r^-$ when $sign(F'_A) > 0$ or if $F'_A \in \pi_r^+$ when $sign(F'_A) < 0$.

Motion ambiguities may arise when the sticking region π_r^0 contains the line π'_t. Then, there are some directions that can cause a break of contact because they do not satisfy the maintenance condition, but at the same time they can produce a sticking at the contact point because they belong to the sticking region. This occurs under some special conditions [38] (e.g. when the reference point of the manipulated object is far away from the contact point and almost above it, being the friction coefficient big enough).

As an example, Figure 2.25 shows several applied forces that produce:

F'_{A_1} : loose of contact.

F'_{A_2} : contact maintenance, positive rotation about the contact point, sliding in the direction $-\vec{t_p}$.

F'_{A_3} : contact maintenance, negative rotation about the contact point, sliding in the direction $-\vec{t_p}$.

F'_{A_4} : contact maintenance, positive rotation about the contact point, sliding in the direction $\vec{t_p}$.

F'_{A_5} : contact maintenance, negative rotation about the contact point, sliding in the direction $\vec{t_p}$.

Therefore, the dual plane can be partitioned in five regions depending on the motion it produces to the manipulated object (Figure 2.26):

Region I: negative rotation about the contact point (R^-), positive sliding (S^+)

Region II: positive rotation about the contact point (R^-), positive sliding (S^+)

Region III: positive rotation about the contact point (R^-), negative sliding (S^+)

Region IV: negative rotation about the contact point (R^-), negative sliding (S^+)

Region V: sticking region.

This partition can be obtained by the following algorithm:

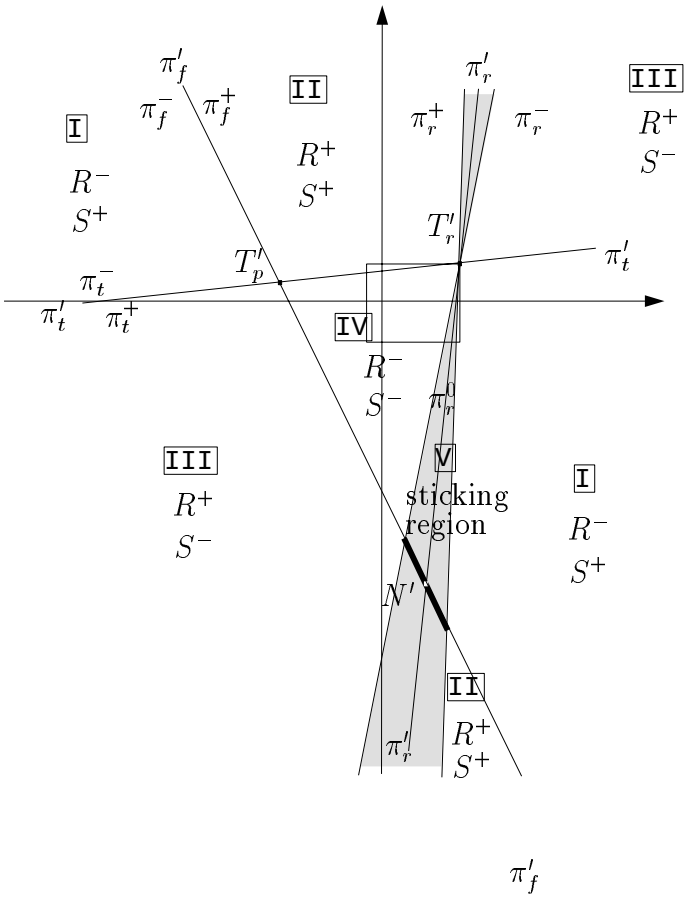

Figure 2.26: *Dual Space Partition*

Dual-plane-partition()

(1) Compute T'_r as the contact point (property 8)

(2) Compute π'_f as the dual line of T'_r (property 9)

(3) Compute π'_t as the line that contains the point T'_r and its direction is $\vec{n}_0$

(4) Compute N' as the dual point of π'_t

(5) Compute the dual friction cone as the dual segment of the cone with vertex at T'_r and directions included in the physical friction cone.

(6) Compute T'_p as the intersection point of lines π'_f and π'_t.

(7) Compute π'_r as the dual line of T'_p

(8) Compute the sticking region as the cone determined by the lines that contain T'_r and one of the extremes of the dual friction cone.

END

In step (4), the point N' can also be computed as the intersection point of π'_f and the line that expresses the direction $\vec{n}_0$ normal to the contact edge (the line perpendicular to $\vec{n}_0$ through the origin). In step (7), the line π'_r can also be computed as the line that contains the points N' and T'_r.